Testability of the type I seesaw mechanism at the CERN LHC: Revealing the existence of the $B - L$ symmetry

Pavel Fileviez Pérez,[1,*] Tao Han,[1,2,†] and Tong Li[2,‡]

[1]*Department of Physics, University of Wisconsin, Madison, Wisconsin 53706, USA*
[2]*Center for High Energy Physics, Peking University, Beijing 100871, People's Republic of China*

(Received 1 August 2009; published 29 October 2009)

We study the possibility to test the type I seesaw mechanism for neutrino masses at the CERN Large Hadron Collider. The inclusion of three generations of right-handed neutrinos (N_i) provides an attractive option of gauging the $B - L$ accidental symmetry in the standard model (as well as an extended symmetry $X = Y - 5(B - L)/4$). The production mechanisms for the right-handed neutrinos through the Z' gauge boson in the $U(1)_{B-L}$ and $U(1)_X$ extensions of the standard model are studied. We discuss the flavor combinations of the charged leptons from the decays of N_i in the $\Delta L = 2$ channels. We find that the clean channels with dilepton plus jets and possible secondary vertices of the N decay could provide conclusive signals at the LHC in connection with the hierarchical pattern of the light neutrino masses and mixing properties within the type I seesaw mechanism.

DOI: 10.1103/PhysRevD.80.073015 PACS numbers: 14.60.St, 13.85.Qk

I. INTRODUCTION

The small but nonzero neutrino masses lead to a deep conjecture: Majorana nature of the neutrino masses may hold the key for a fundamentally different mass generation mechanism, although Dirac masses can be generated via the Higgs mechanism by introducing right-handed neutrinos with arbitrarily small Yukawa couplings. There are three simple scenarios where one can generate Majorana masses of the neutrinos with renormalizable operators at tree level, and in agreement with the observations, the type I [1], type II [2], and type III [3] seesaw mechanisms. See also Refs. [4,5] for the simplest neutrino mass generation mechanisms using radiative corrections.

Perhaps the simplest and best-studied mechanism for neutrino masses is the type I seesaw, where one introduces at least two right-handed neutrinos (N). Adding in the corresponding large Majorana mass terms (M), one finds at least two light Majorana neutrinos with masses given as m_D^2/M. It is important to mention that the inclusion of three right-handed neutrinos also provides an anomaly-free formulation for a gauged $U(1)_{B-L}$ [6].

The nonambiguous test of the Majorana nature of the neutrinos, and thus a possible test of the seesaw mechanism, will be the observation of the lepton number violation processes. The neutrinoless double beta decay is also a crucial test and one of the most sensitive probes. Since the CERN Large Hadron Collider (LHC) is going to lead us to a new energy frontier, searching for the heavy Majorana neutrinos at the LHC appears to be very appealing [7,8]. However, due to the rather small mixing between the heavy neutrinos and the standard model (SM) leptons in a minimal type I scheme, typically of the order $|V_{\ell N}|^2 \sim m_\nu/M_N$, the predicted effects of lepton number violation are unlikely to be observable. On the other hand, if there are other particles beyond the SM that can mediate new interactions between them, the effects may be significantly enhanced. For instance, with the new gauge interaction $U(1)_{B-L}$, the gauge boson Z_{B-L} can be produced copiously at the LHC via its gauge interactions with the quarks. Its subsequent decay to a pair of heavy Majorana neutrinos may lead to a large sample of events without involving the small mixing angle suppression of N [9,10]. The $\Delta L = 2$ signals will directly test its Majorana nature; and the lepton flavor combination could probe the properties of the light neutrino mass spectrum and mixing pattern.

In this paper, we investigate the possibility to test the type I seesaw mechanism at the LHC in the context of two simple extensions of the standard model where one has an extra Abelian gauge symmetry. We focus our attention on scenarios with a $U(1)_{B-L}$ or $U(1)_X (X = Y - 5(B - L)/4)$, where B, L, and Y stand for baryon number, lepton number, and weak hypercharge, respectively. In order to cancel the anomalies, one just needs to introduce three right-handed neutrinos, which are the source for the Majorana masses. In both scenarios one has a new neutral gauge boson, Z', which couples to the right-handed neutrinos. Then, one can expect a large number of lepton number violating events due to the production and decays of the TeV Majorana neutrinos. The predictions of the heavy neutrino decays in each neutrino spectrum, normal hierarchy (NH), inverted hierarchy (IH) or quasidegenerate (QD), are investigated in great detail. We find encouraging results for the LHC signatures to learn about the light neutrino properties.

This work is organized as follows: In Sec. II we discuss the constraints on the mass and mixing parameters in the type I seesaw mechanism from the current neutrino oscil-

*fileviez@physics.wisc.edu
†than@hep.wisc.edu
‡nklitong@hotmail.com, communication author

lation data. The predictions for the decays of the heavy neutrinos in the different neutrino spectra are presented in Sec. III. In Sec. IV we discuss the possibility to test type I seesaw at the LHC through the same-sign dilepton channels. We summarize our findings in Sec. V. The mixing between light and heavy neutrinos is discussed in Appendix A. We provide the explicit expressions for these mixings in Appendix B. The minimal extensions of the standard model to $U(1)_{B-L}$ and $U(1)_X$ are discussed in Appendix C.

II. TYPE I SEESAW MECHANISM AND PARAMETER CONSTRAINTS

In the case of the type I seesaw mechanism for neutrino masses one introduces at least two SM singlets, right-handed neutrinos, $\nu_R \sim (1, 1, 0)$, in order to generate two nonzero neutrino masses. In this case the relevant Yukawa interaction and the Majorana mass term are given by

$$-\mathcal{L}_\nu^I = Y_\nu^D \bar{l}_L \tilde{H} \nu_R + \frac{M_N}{2} \nu_R^T C \nu_R + \text{H.c.} \tag{1}$$

Here $\tilde{H} = i\sigma_2 H^*$ and the lepton number is broken in two units due to the presence of both terms. Now, integrating out the right-handed neutrinos one finds that the mass matrix for the light neutrinos is given by

$$M_\nu = m_D M_N^{-1} m_D^T, \tag{2}$$

where $m_D = Y_\nu^D v_0/\sqrt{2}$ is the Dirac mass term and v_0 is the Higgs vacuum expectation value. Therefore, in this framework one could understand the smallness of neutrino masses, since the mass scale M_N in the above equation could be large, $M_N \gg Y_\nu^D v_0$, This is the so-called canonical type I seesaw mechanism [1]. The mass matrix for neutrinos is diagonalized by unitary rotations as detailed in Appendix A. The three light neutrino masses can be expressed in the following way:

$$m = V_{\text{PMNS}}^\dagger M_\nu V_{\text{PMNS}}^*, \tag{3}$$

where $m = \text{diag}(m_1, m_2, m_3)$ and V_{PMNS} can be taken as the leptonic Pontecorvo-Maki-Nakagawa-Sakata (PMNS) mixing matrix for the three generations of light neutrinos [11] without the loss of generality.[1] Working in the basis where the heavy neutrino mass matrix is diagonal and using the Casas-Ibarra parametrization [12] one can write m_D satisfying Eq. (2) as

$$m_D = V_{\text{PMNS}} m^{1/2} \Omega M^{1/2}, \tag{4}$$

where $M = \text{diag}(M_1, M_2, M_3)$ for heavy neutrino masses, and Ω is a complex matrix which satisfies the orthogonality condition $\Omega^T \Omega = 1$. It is shown in Appendix A that using the seesaw formula and the relation between the leptonic mixing one can find a formal solution for the mixing between the SM charged leptons ($\ell = e, \mu, \tau$) and heavy neutrinos ($N = 1, 2, 3$):

$$V_{\ell N} = V_{\text{PMNS}} m^{1/2} \Omega M^{-1/2}. \tag{5}$$

Therefore, for a given form of Ω, one can establish the connection between the heavy neutrino decays and the properties of the light neutrinos. The impact of the existence of the Ω matrix on the decays of heavy neutrinos has not been studied before in collider phenomenology. Unfortunately, since the explicit form of this matrix is unknown one cannot predict the decay pattern of the heavy neutrinos with respect to the spectrum for light neutrinos. We will present a few well-motivated typical cases where one can hope to see the connection in each spectrum for light neutrinos. It is important, however, to realize that an underlying theory would pick only one specific form of Ω. This (yet unknown) form would have definite prediction for the N decay patterns, through which the underlying theory could be revealed.

A. Constraints on the physical parameters

1. Neutrino masses and mixings

In order to understand the constraints coming from neutrino physics let us discuss the relation between the neutrino masses and mixing. The leptonic mixing matrix is given by

$$V_{\text{PMNS}} = \begin{pmatrix} c_{12}c_{13} & c_{13}s_{12} & e^{-i\delta}s_{13} \\ -c_{12}s_{13}s_{23}e^{i\delta} - c_{23}s_{12} & c_{12}c_{23} - e^{i\delta}s_{12}s_{13}s_{23} & c_{13}s_{23} \\ s_{12}s_{23} - e^{i\delta}c_{12}c_{23}s_{13} & -c_{23}s_{12}s_{13}e^{i\delta} - c_{12}s_{23} & c_{13}c_{23} \end{pmatrix} \times \text{diag}(e^{i\Phi_1/2}, 1, e^{i\Phi_2/2}), \tag{6}$$

where $s_{ij} = \sin\theta_{ij}$, $c_{ij} = \cos\theta_{ij}$, $0 \le \theta_{ij} \le \pi/2$, and $0 \le \delta \le 2\pi$. The phase δ is the Dirac CP phase, and Φ_i are the Majorana phases. The experimental constraints on the neutrino masses and mixing parameters, at 2σ level [13], are

$$7.25 \times 10^{-5}\ \text{eV}^2 < \Delta m_{21}^2 < 8.11 \times 10^{-5}\ \text{eV}^2, \tag{7}$$

$$2.18 \times 10^{-3}\ \text{eV}^2 < |\Delta m_{31}^2| < 2.64 \times 10^{-3}\ \text{eV}^2, \tag{8}$$

$$0.27 < \sin^2\theta_{12} < 0.35, \tag{9}$$

$$0.39 < \sin^2\theta_{23} < 0.63, \tag{10}$$

[1]The 3×3 rotational matrix is not exactly unitary when there are extra Majorana neutrinos, but it is a good approximation to equal it to the traditional V_{PMNS}; see the formalism in Appendix A.

$$\sin^2\theta_{13} < 0.040, \tag{11}$$

and $\sum_i m_i < 1.2$ eV. For a complete discussion of these constraints see Ref. [14]. Following the convention, we denote the case $\Delta m^2_{31} > 0$ as the normal hierarchy (NH), $\Delta m^2_{31} < 0$ the inverted hierarchy (IH), and the quasidegenerate (QD) spectrum where the lightest neutrino mass is larger than 5×10^{-2} eV. Using the above experimental constraints, one can expect to explore the allowed values for the $V_{\ell N}$ couplings and the heavy masses. From Eq. (5), we can obtain the general expressions of $\sum_N (V^*_{\ell N})^2$ that are collected in Appendix B.

2. Case I: Degenerate heavy neutrinos

We first study the simplest case where the three heavy neutrinos are degenerate. This is a highly motivated scenario since it is strongly favored to generate successful resonant leptogenesis [15,16] at the low scale. Using Eq. (A15) and assuming degenerate heavy neutrinos we obtain the relation

$$M \sum_{N=1,2,3} (V^*_{\ell N})^2 = (V^*_{\rm PMNS} m V^\dagger_{\rm PMNS})_{\ell\ell} \equiv (M_\nu)_{\ell\ell}, \quad (\ell = e, \mu, \tau). \tag{12}$$

We see that one can obtain simple relations for the heavy neutrino mixings and masses in terms of the light neutrino mass matrix independent of the unknown matrix Ω, which in turn is given by the parameters from the neutrino oscillation data. One can thus predict the decays of the heavy neutrinos in each spectrum for light neutrinos. Note that in this degenerate scenario, we are unable to convert the constraints of Eq. (12) to predict $\sum_N |V_{\ell N}|^2$ in general. We can predict the decays of heavy neutrinos in terms of the other oscillation parameters only when all phases vanish since in this case the modulo square of the mixings (which govern the decay rate) are equal to the square of mixings [the left-handed side of Eq. (12)].

In Ref. [17], we have shown that, using the experimental constraints on the neutrino mass parameters, the elements of the neutrino mass matrix have the following properties:

$$\begin{aligned} M^{ee}_\nu &\ll M^{\mu\mu}_\nu, \quad M^{\tau\tau}_\nu \quad \text{for NH,} \\ M^{ee}_\nu &> M^{\mu\mu}_\nu, \quad M^{\tau\tau}_\nu \quad \text{for IH,} \end{aligned} \tag{13}$$

$$M^{ee}_\nu \approx M^{\mu\mu}_\nu \approx M^{\tau\tau}_\nu \quad \text{for QD.} \tag{14}$$

Following the same approach, we plot the allowed values for the normalized couplings of each lepton flavor in this scenario in Fig. 1, as a function of the lightest neutrino mass in each spectrum, the normal hierarchy (left panel) and the inverted hierarchy (right panel), assuming vanishing Majorana phases. We see two distinctive regions in terms of the lightest neutrino mass as expected. In the case $m_{1(3)} < 5 \times 10^{-2}$ eV, we see the characteristic features

$$\begin{aligned} \sum_N |V_{eN}|^2 &\ll \sum_N |V_{\mu N}|^2, \quad \sum_N |V_{\tau N}|^2 \quad \text{for NH,} \\ \sum_N |V_{eN}|^2 &> \sum_N |V_{\mu N}|^2, \quad \sum_N |V_{\tau N}|^2 \quad \text{for IH.} \end{aligned}$$

On the other hand, for $m_{1(3)} > 5 \times 10^{-2}$ eV, the light neutrino masses enter the QD spectrum that leads to

$$\sum_N |V_{eN}|^2 \approx \sum_N |V_{\mu N}|^2 \approx \sum_N |V_{\tau N}|^2.$$

Under this mass degenerate assumption, the mixing between the heavy neutrinos and the SM charged leptons simply reflects the features of the light neutrino mass matrix in the flavor basis, as seen in Eq. (12). This is an important model prediction. It is important to emphasize that the results shown in Fig. 1 may be used to learn about the neutrino spectrum.

3. Case II: Nondegenerate heavy neutrinos

If we relax the assumption that heavy Majorana neutrinos are nearly degenerate in mass, then the complication

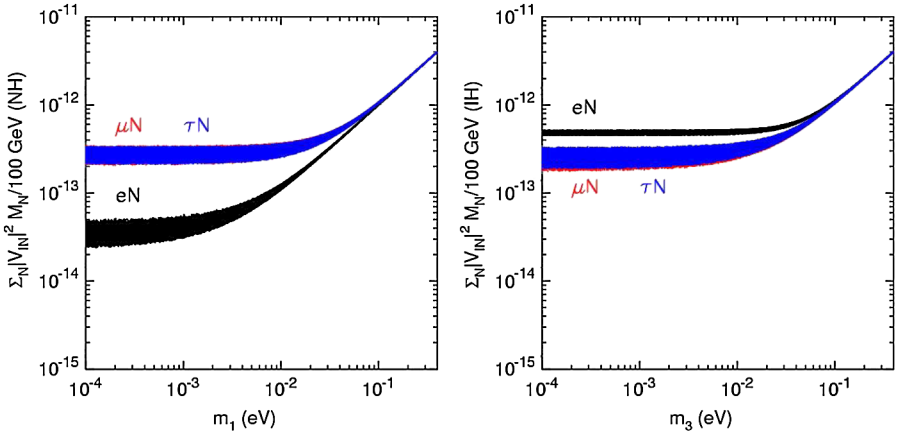

FIG. 1 (color online). $\sum_N |V_{\ell N}|^2 M_N/100$ GeV versus the lightest neutrino mass for NH (left) and IH (right) in case I (degenerate N), assuming vanishing Majorana phases.

due to the unknown matrix Ω arises. The explicit parametrization of Ω is presented in Appendix A, and the general expressions for the relations among the parameters are given in Appendix B.

For the purpose of illustration, let us take Ω to be a real matrix. We could gain a general sense for the mixing parameters by varying the matrix elements of Ω in the range of $-1 \leq w_{ij} \leq 1$. We show $|V_{\ell 1}|^2 M_1/100$ GeV in this case in Fig. 2. The predictions of $|V_{\ell 2}|^2 M_2/100$ GeV and $|V_{\ell 3}|^2 M_3/100$ GeV are almost the same. As one can see, qualitative features for both cases of NH and IH closely resemble those in Fig. 1. This is quite encouraging since the random selection of the model parameters does not seem to totally wash out the predicted features. To further explore the model implications, we must choose a specific form of the Ω matrix, which should correspond to a particular theoretical incarnation in the right-handed neutrino sector. However, a large Majorana phase could alter the predictions [17] in general. We will check on this point in the next section.

Case IIa: $\Omega = I$.—In this simple scenario, we easily obtain transparent relations for the N_1 mixings,

$$|V_{e1}|^2 M_1 = m_1 c_{12}^2 c_{13}^2 \approx m_1 c_{12}^2, \tag{15}$$

$$|V_{\mu 1}|^2 M_1 = m_1 |s_{12} c_{23} + c_{12} s_{13} s_{23} e^{i\delta}|^2 \approx m_1 s_{12}^2 c_{23}^2, \tag{16}$$

$$|V_{\tau 1}|^2 M_1 = m_1 |s_{12} s_{23} - c_{12} s_{13} c_{23} e^{i\delta}|^2 \approx m_1 s_{12}^2 s_{23}^2, \tag{17}$$

and therefore $|V_{e1}|^2 > |V_{\mu 1}|^2, |V_{\tau 1}|^2$. In the case of N_2 mixing,

$$|V_{e2}|^2 M_2 = m_2 c_{13}^2 s_{12}^2 \approx m_2 s_{12}^2, \tag{18}$$

$$|V_{\mu 2}|^2 M_2 = m_2 |c_{12} c_{23} - s_{12} s_{13} s_{23} e^{i\delta}|^2 \approx m_2 c_{12}^2 c_{23}^2, \tag{19}$$

$$|V_{\tau 2}|^2 M_2 = m_2 |s_{12} s_{13} c_{23} e^{i\delta} + c_{12} s_{23}|^2 \approx m_2 c_{12}^2 s_{23}^2, \tag{20}$$

and $|V_{e2}|^2 \approx |V_{\mu 2}|^2 \approx |V_{\tau 2}|^2$. As for the N_3 mixing,

$$|V_{e3}|^2 M_3 = m_3 s_{13}^2 \approx 0, \tag{21}$$

$$|V_{\mu 3}|^2 M_3 = m_3 c_{13}^2 s_{23}^2 \approx m_3 s_{23}^2, \tag{22}$$

$$|V_{\tau 3}|^2 M_3 = m_3 c_{13}^2 c_{23}^2 \approx m_3 c_{23}^2, \tag{23}$$

and one can see $|V_{\mu 3}|^2, |V_{\tau 3}|^2 > |V_{e3}|^2$. These features are shown in Fig. 3.

A few remarks are in order. First of all, with this choice of a diagonal matrix Ω, the mixing angle squared $|V_{\ell i}|^2$ for N_i is always proportional to the corresponding light neutrino mass m_i. Consequently, the relative fractions of the mixing to different lepton flavors are universal for both NH and IH. Second, the Majorana phases do not appear in $|V_{\ell N}|^2$ due to the special structure of Ω. Third, as seen in Fig. 3, the relative strength of the mixing to different lepton flavors for each N_i closely follows that for the light neutrino mass eigenstates. In fact, very much like the light neutrino mass eigenstate labeling, this should be the defining feature to label N_1, N_2, and N_3, if we do not like the less illuminating ordering $M_1 < M_2 < M_3$.

Case IIb: $\Omega = I_{\text{off}}$.—We choose to study yet another simple but different form of the matrix, namely, with Ω as an off-diagonal unity matrix. As can be shown explicitly and supported by Fig. 4, the mixing features of $|V_{\ell 1}|^2$ and $|V_{\ell 3}|^2$ switch places with each other in both NH and IH, while $|V_{\ell 2}|^2$ remain the same as in the $\Omega = I$ case. If we recall the convention for the N_i labeling, this case is indistinguishable from case IIa. In this case $|V_{\ell N}|^2$ are also independent of Majorana phases. This similarity can be

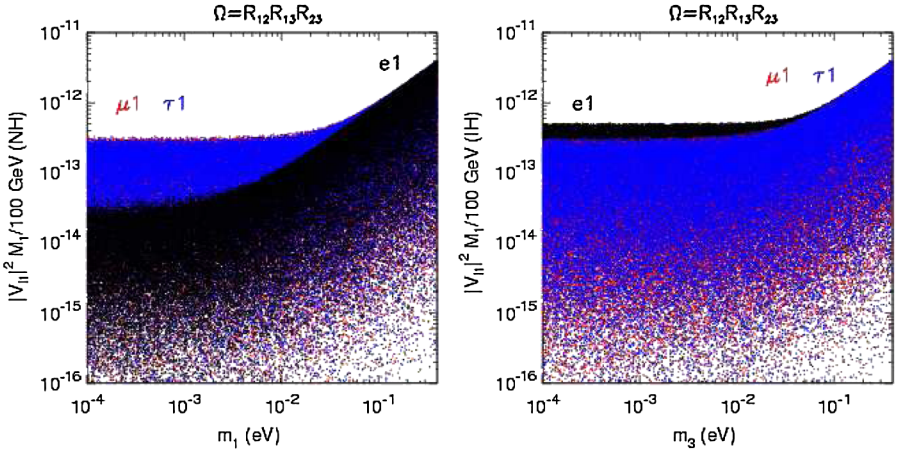

FIG. 2 (color online). $|V_{\ell 1}|^2 M_1/100$ GeV versus the lightest neutrino mass for NH (left) and IH (right) with $\Omega = R_{12} R_{13} R_{23}$ and random matrix elements $-1 \leq w_{ij} \leq 1$, assuming vanishing Majorana phases.

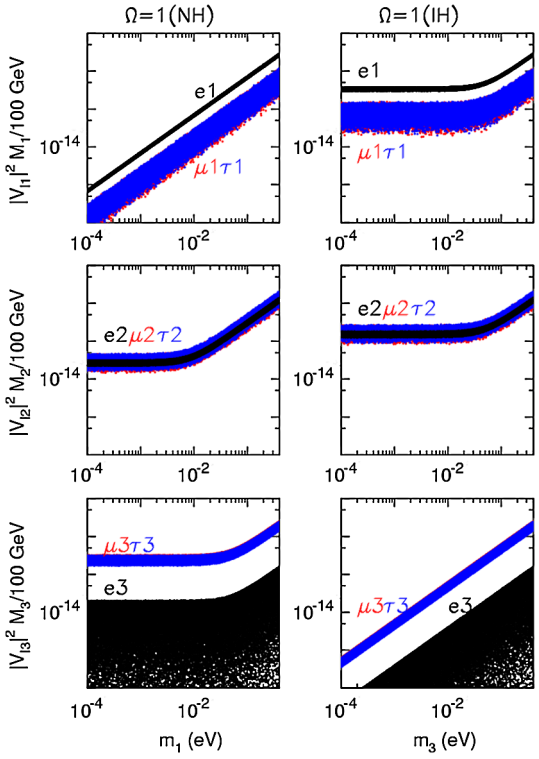

FIG. 3 (color online). $|V_{\ell i}|^2 M_i/100$ GeV, $i = 1, 2, 3$ versus the lightest neutrino mass for NH (left panels) and IH (right panels) in case IIa ($\Omega = I$).

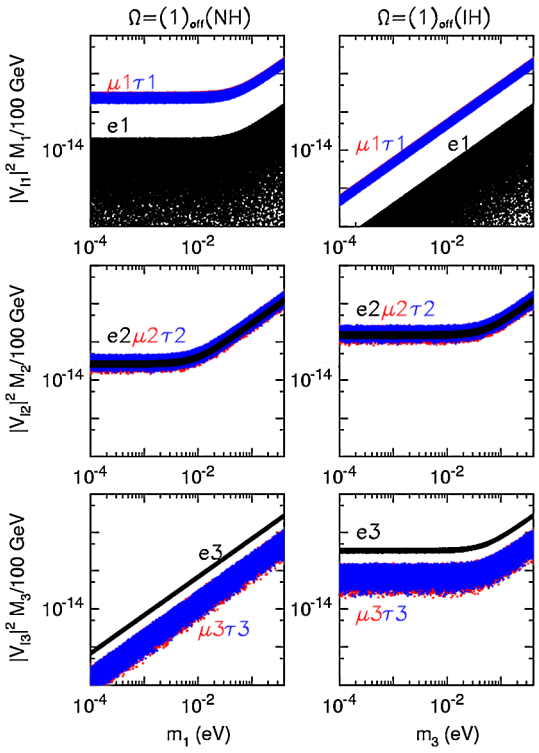

FIG. 4 (color online). $|V_{\ell i}|^2 M_i/100$ GeV, $i = 1, 2, 3$ versus the lightest neutrino mass for NH (left panels) and IH (right panels) in case IIb ($\Omega = I_{\rm off}$).

generalized to a matrix of Ω which has only unity as entries. We would expect that the real situation could be a well-defined superposition of the three vertical panels as long as Ω is real.

III. HEAVY NEUTRINO DECAYS AND LIGHT NEUTRINO SPECTRA

The leading decay channels for the heavy neutrinos include $N_i \to e_j^{\pm} W^{\mp}$, $N_i \to \nu_j Z$, and $N_i \to \nu_j h(H)$. The amplitudes for the two first channels are proportional to the mixing between the leptons and heavy neutrinos given in Eq. (5), while the last one is proportional to the Dirac-like Yukawa terms given in Eq. (4).

A. Decay modes of heavy Majorana neutrinos with mass: $M_i > M_W$

The partial decay widths of the heavy Majorana neutrinos N_i are given by

$$\Gamma^{\ell W_L} \equiv \Gamma(N_i \to \ell^- W_L^+) = \Gamma(N_i \to \ell^+ W_L^-) = \frac{g^2}{64\pi M_W^2} |V_{\ell i}|^2 M_i^3 (1 - \mu_{iW})^2, \tag{24}$$

$$\Gamma^{\ell W_T} \equiv \Gamma(N_i \to \ell^- W_T^+) = \frac{g^2}{32\pi} |V_{\ell i}|^2 M_i (1 - \mu_{iW})^2, \tag{25}$$

$$\Gamma^{\nu_\ell Z_L} \equiv \Gamma(N_i \to \nu_\ell Z_L) = \frac{g^2}{64\pi M_W^2} |V_{\ell i}|^2 M_i^3 (1 - \mu_{iZ})^2, \tag{26}$$

$$\Gamma^{\nu_\ell Z_T} \equiv \Gamma(N_i \to \nu_\ell Z_T) = \frac{g^2}{32\pi c_W^2} |V_{\ell i}|^2 M_i (1 - \mu_{iZ})^2, \tag{27}$$

where $\mu_{ij} = M_j^2/M_i^2$. If N_i is heavier than the Higgs bosons h and H (see Appendix C for the properties of the Higgs bosons in the $B - L$ extension of the SM), one has the additional channels

$$\Gamma^{\nu_\ell h} \equiv \Gamma(N_i \to \nu_\ell h) = \frac{g^2}{64\pi M_W^2} |V_{\ell i}|^2 M_i^3 (1 - \mu_{ih})^2 \cos^2\theta_0, \tag{28}$$

$$\Gamma^{\nu_\ell H} \equiv \Gamma(N_i \to \nu_\ell H) = \frac{g^2}{64\pi M_W^2} |V_{\ell i}|^2 M_i^3 (1 - \mu_{iH})^2 \sin^2\theta_0. \tag{29}$$

Therefore, the total width for N_i is given by

$$\Gamma_{N_i} = \sum_\ell (2\Gamma^{\ell W_L} + 2\Gamma^{\ell W_T} + \Gamma^{\nu_\ell Z_L} + \Gamma^{\nu_\ell Z_T} + \Gamma^{\nu_\ell h} + \Gamma^{\nu_\ell H}). \tag{30}$$

At a high mass of M_N, the branching ratios of the leading channels go like

$$\Gamma(\ell^- W_L^+) \approx \Gamma(\ell^+ W_L^-) \approx \Gamma(\nu Z_L) \approx \Gamma(\nu h + \nu H). \quad (31)$$

As discussed above, the lepton flavor contents of N decays will be different in each neutrino spectrum. Here, we also study this issue in great detail for cases I and II. In order to search for the events with best reconstruction, we will only consider the N decay to charged leptons plus a $W^\pm$.

1. Decays in Case I: Degenerate heavy neutrinos

In Fig. 5 we show the impact of the neutrino masses and mixing angles on the branching fractions of the sum of the degenerate neutrinos N_i, $i = 1, 2, 3$ decaying into e, μ, τ lepton plus W boson, respectively, with the left panels for the normal hierarchy (NH) and the right panels of the inverted hierarchy (IH), assuming vanishing Majorana phases. Qualitatively, it follows the relations in Eq. (14)

$$\begin{aligned} &\mathrm{BR}(\mu^\pm W^\mp), \qquad \mathrm{BR}(\tau^\pm W^\mp) \gg \mathrm{BR}(e^\pm W^\mp) \quad \text{for NH,} \\ &\mathrm{BR}(e^\pm W^\mp) > \mathrm{BR}(\mu^\pm W^\mp), \qquad \mathrm{BR}(\tau^\pm W^\mp) \quad \text{for IH.} \end{aligned} \quad (32)$$

The branching fraction can differ by 1 order of magnitude in the NH case; and about a factor of few in the IH spectrum. As one expects that all these channels are quite similar when the neutrino spectrum is quasidegenerate, $m_1 \approx m_2 \approx m_3 \geq 0.05$ eV. Therefore, in this simple case one can hope that if the heavy neutrino decays are observed in future experiments one should be able to distinguish the neutrino spectrum.

Decays in Case II: Nondegenerate heavy neutrinos

For nondegenerate neutrino spectra we once again study the simple choice: case IIa $\Omega = I$. We show the branching fractions of processes $N_i \to \ell^+ W^- + \ell^- W^+$ ($\ell = e, \mu, \tau$, $i = 1, 2, 3$) corresponding to the lightest neutrino mass for NH and IH for $M_i = 300$ GeV in Fig. 6. As noted earlier, in this simplest case all $|V_{\ell i}|^2$ ($\ell = e, \mu, \tau$) are proportional to m_i. Therefore the branching ratio of $N_i \to \ell^\pm W^\mp$ for each lepton flavor is independent of neutrino mass and thus universal for both NH and IH. Although we cannot distinguish the neutrino mass hierarchy, we still can tell the

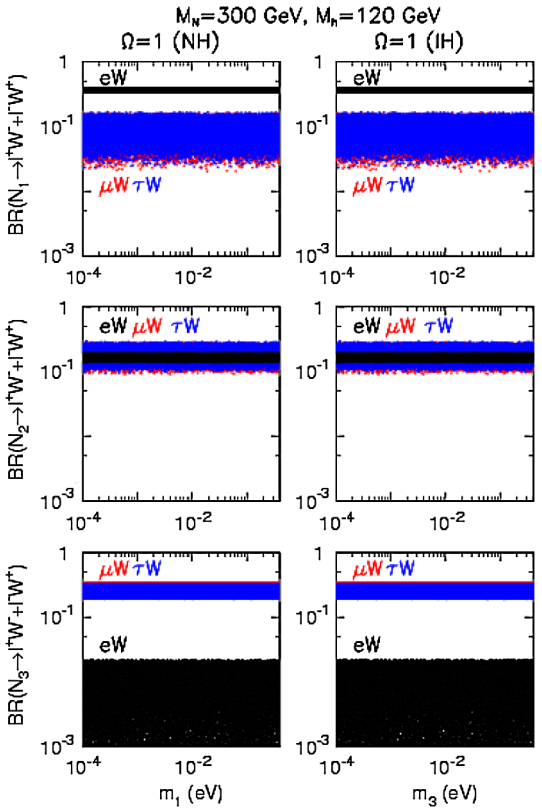

FIG. 6 (color online). Branching fractions of process $N_i \to \ell^+ W^- + \ell^- W^+$ ($\ell = e, \mu, \tau$, $i = 1, 2, 3$) versus the lightest neutrino mass for NH and IH in case IIa ($\Omega = I$), when $M_i = 300$ GeV and $M_h = 120$ GeV.

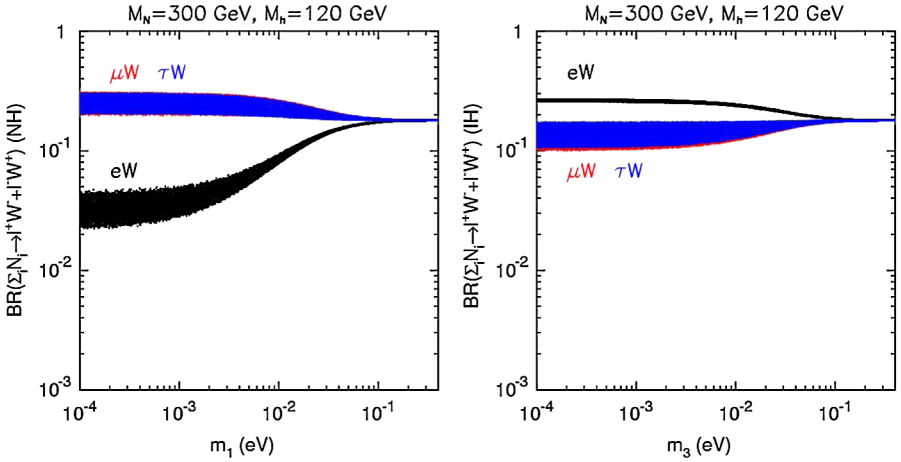

FIG. 5 (color online). Branching fractions of degenerate neutrinos $\sum_i N_i \to \ell^+ W^- + \ell^- W^+$ ($\ell = e, \mu, \tau$) for NH and IH versus lightest neutrino mass with $M_N = 300$ GeV and $M_h = 120$ GeV, assuming vanishing Majorana phases.

difference of the three heavy Majorana neutrinos according to different SM lepton flavors in final states of their dominant decay channels. One has

$$\mathrm{BR}(e^{\pm}W^{\mp}) > \mathrm{BR}(\mu^{\pm}W^{\mp}), \quad \mathrm{BR}(\tau^{\pm}W^{\mp}) \quad \text{for } N_1,$$
$$\mathrm{BR}(e^{\pm}W^{\mp}) \approx \mathrm{BR}(\mu^{\pm}W^{\mp}) \approx \mathrm{BR}(\tau^{\pm}W^{\mp}) \quad \text{for } N_2,$$
$$\mathrm{BR}(\mu^{\pm}W^{\mp}), \quad \mathrm{BR}(\tau^{\pm}W^{\mp}) \gg \mathrm{BR}(e^{\pm}W^{\mp}) \quad \text{for } N_3.$$

This follows closely to the mixing strengths of the light neutrinos in the previous section.

As discussed previously, case IIb $\Omega = I_{\mathrm{off}}$ is identical to the above if we identify $N_1 \leftrightarrow N_3$. A more involved case for Ω may be some form of superposition of the three decay patterns, that is to be tested experimentally by the flavor combinations.

B. Impact of Majorana phases in heavy Majorana neutrino decays

In our previous discussion we have shown that the mixings $|V_{\ell N}|^2$ are independent of Majorana phases in both case IIa and IIb (as well for an Ω with unity as entries). In general, the N_i decay rates depend on only one Majorana phase $\Phi_2(\Phi_1)$ when $m_{1(3)} \approx 0$ and $s_{13} = 0$ in the NH (IH) case as shown explicitly in the appendixes. In Fig. 7, we show the dependence of N_1 decay branching fractions for a general nondegenerate case on Majorana phases Φ_2 and Φ_1 in NH and IH, with random selection of the Ω matrix elements. The dependence of N_2 and N_3 decays on Majorana phases is almost the same as that of N_1. The branching fractions of $\mu^{\pm}W^{\mp}$, $\tau^{\pm}W^{\mp}$ ($e^{\pm}W^{\mp}$) are typically dominant over all the range of Φ_2 (Φ_1) in NH (IH). The dependence on the phases for the leading channels is rather weak and it is thus hard to extract the phase information from heavy Majorana neutrino decay. Some typical situations may be similar to the cases discussed in Ref. [17], and we will not pursue further for the phase effects.

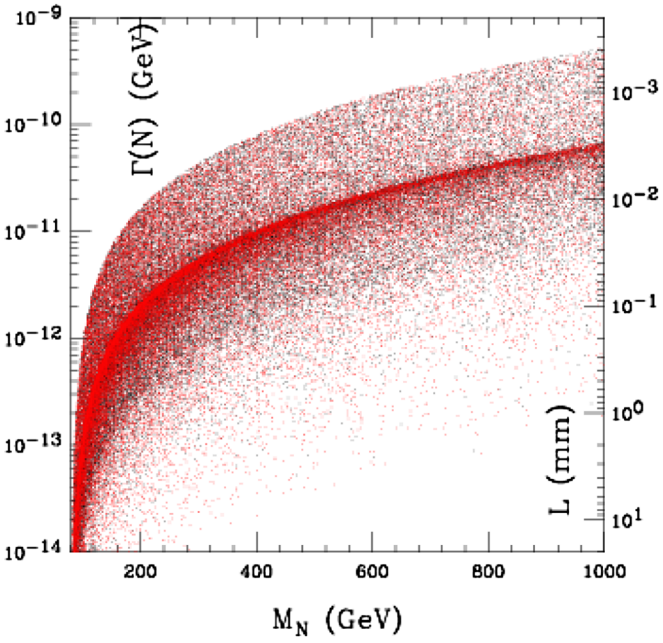

FIG. 8 (color online). The total width and decay length of N in the general nondegenerate case, when the lightest neutrino mass 10^{-4} eV $\leq m_{1(3)} \leq 0.4$ eV, $M_h = 120$ GeV, and $\Omega = R_{12}R_{13}R_{23}$ with random selection of the matrix elements and.

C. Total decay width of heavy Majorana neutrino

To complete this section about the heavy Majorana neutrino properties, we study their total decay widths, which are proportional to $M_\nu M_N^2/M_W^2$. In Fig. 8, we plot the total width (left axis) and decay length (right axis) for N versus M_N under the general nondegenerate case with random selection of the Ω matrix elements (similar for NH and IH). There is a large spread for the possible ranges of the decay lengths, governed by the mixing parameters. Although not generally considered as long-lived for large mass, the N decay lengths may be typically in the range of

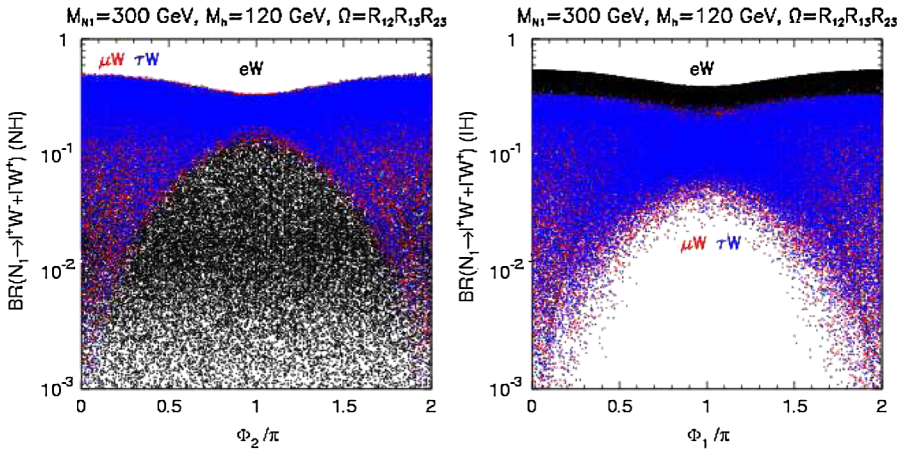

FIG. 7 (color online). Branching fractions of $N_1 \to \ell^+W^- + \ell^-W^+$ versus Majorana phase Φ_2 for NH and Φ_1 for IH in the general nondegenerate case when $M_1 = 300$ GeV, $M_h = 120$ GeV, with random selection of the Ω matrix elements.

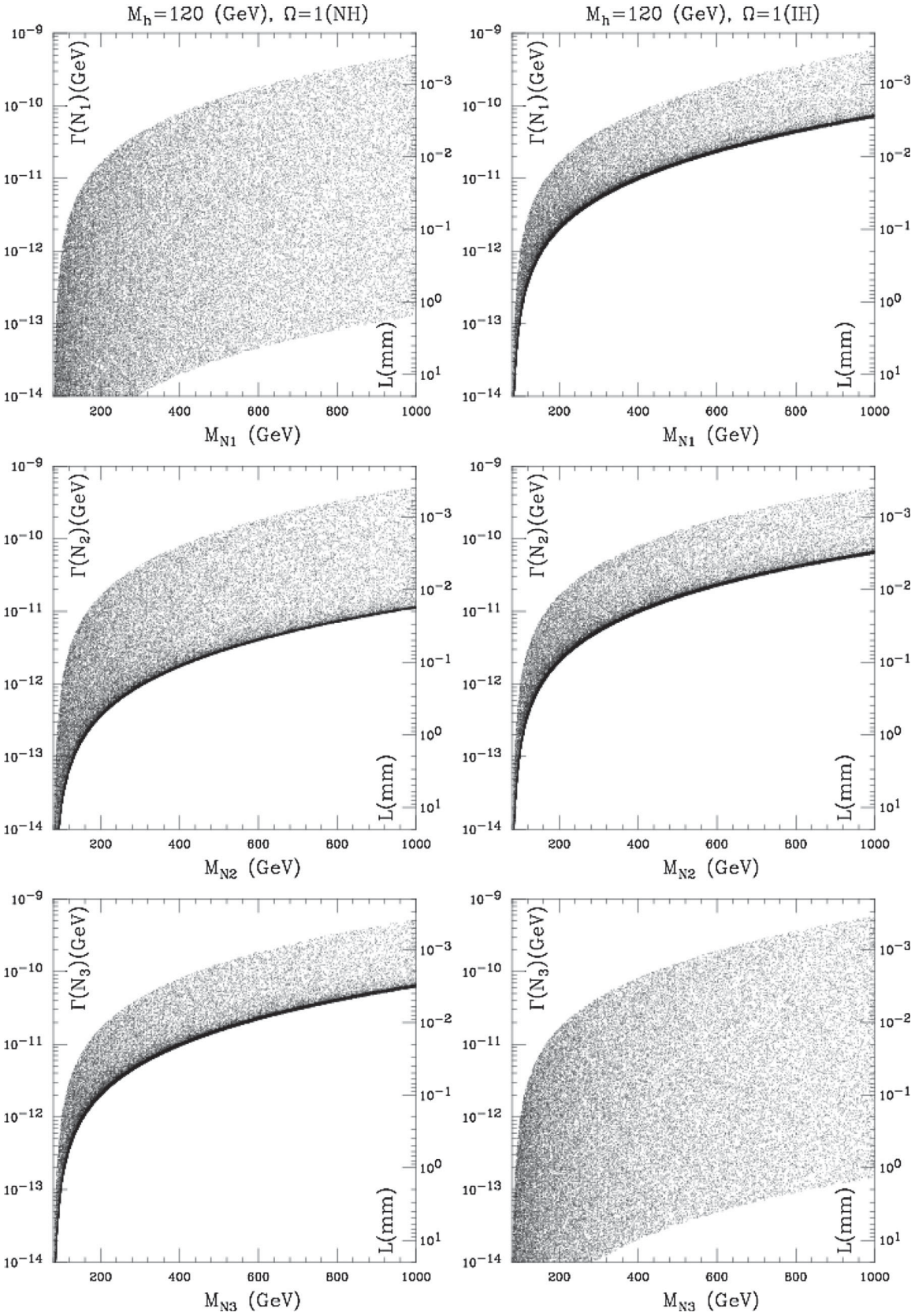

FIG. 9. Total width and decay length of $N_i (i = 1, 2, 3)$ for NH and IH in case IIa ($\Omega = I$), when the lightest neutrino mass 10^{-4} eV $\leq m_{1(3)} \leq 0.4$ eV and $M_h = 120$ GeV.

μm–cm, and their decays could lead to a visible displaced vertex in the detector at the LHC.

When considering a specific model-parameter setting, we plot the total width (left axis) and decay length (right axis) in Fig. 9, for N_i versus M_N for $M_h = 120$ GeV in NH and IH under case IIa with $\Omega = I$. One of the generic features for all N_i and both NH and IH is a typical lower limit for their lifetime (or decay length). For instance, the typical decay length for $M_N \gtrsim 600$ GeV is above 1 μm. For smaller values of M_N, the heavy Majorana neutrinos can be long-lived in the detector scale, making the signatures detectable at the secondary vertex. In fact, this feature remains in a majority part of the parameter space. In particular, because in this case all $|V_{\ell i}|^2$ are proportional to m_i, the lifetimes of N_1 in NH and N_3 in IH could be infinite when neglecting the lightest neutrino mass in the whole Majorana neutrino mass range. It is interesting to note that there is a clear difference between the NH and IH scenarios: the lifetime of N_1 in IH and N_3 in NH has a narrowly predicted range within 1 order of magnitude, about 10 μm for $M_N = 400$ GeV. If this is indeed observed, it could serve as an indication to distinguish the models. The lifetimes of N_2 in NH and IH are almost the same.

For case IIb with an off-diagonal Ω matrix, the lifetime features of N_1 and N_3 are also interchanged with each other and those of N_2 are still the same as case IIa.

IV. HEAVY MAJORANA NEUTRINOS AND THE TEST OF TYPE I SEESAW AT THE LHC

In order to study the prediction for the lepton flavor correlations with heavy Majorana neutrino and its lepton number violation decay processes, the ideal production channels are the Drell-Yan processes via SM gauge bosons, $pp \to W \to N\ell$, $pp \to Z \to NN$. However, the gauge couplings to N are highly suppressed to the order $\mathcal{O}(m_\nu/M_N)$ [8]. The situation is very different in the case of the minimal $B - L$ extension of the SM (see Appendix C) where one can produce the heavy neutrinos through the Z' in the theory.

A. Gauge boson properties: Z'

In the limit where there is no mixing between the two Abelian sectors of the minimal $B - L$ extension of the SM [see Appendix C, $\epsilon = 0$ in Eq. (C3)], the mass of the new gauge boson Z' is given by

$$M_{Z'} = 2 g_{BL} v_S. \tag{33}$$

To satisfy the experimental lower bound, $M_{Z'}/g_{BL} >$ (5–10) TeV, it is sufficient to assume that $v_S >$ 2.5–5 TeV. The relevant interactions to matter are given by

$$g_{BL} Z'_\mu (Q^q_{BL}[\bar{u}\gamma^\mu u + \bar{d}\gamma^\mu d] + Q^\ell_{BL}[\bar{e}\gamma^\mu e + \bar{\nu}_L \gamma^\mu \nu_L + \bar{\nu}_R \gamma^\mu \nu_R]), \tag{34}$$

where the $B - L$ charges are assigned to be $Q^q_{BL} = 1/3$, and $Q^\ell_{BL} = -1$.

There has been a lot of work on the heavy neutral gauge bosons. For a recent review, see Ref. [18], and recent studies of Z' at the Tevatron and LHC [19]. For a recent consideration of the phenomenological aspects of the $B - L$ model, see [9]. The expressions for the possible decays of the Z' are given by

$$\Gamma(Z' \to f\bar{f}) = g^2_{BL} \frac{M_{Z'}}{12\pi} C_f (Q^f_{BL})^2 \left(1 + 2\frac{m_f^2}{M^2_{Z'}}\right)\beta_f, \tag{35}$$

$$\Gamma\left(Z' \to \sum_m \nu_m \nu_m\right) = 3 g^2_{BL} \frac{M_{Z'}}{24\pi} C_\nu (Q^\ell_{BL})^2, \tag{36}$$

$$\Gamma(Z' \to N_m N_m) = g^2_{BL} \frac{M_{Z'}}{24\pi} C_N (Q^\ell_{BL})^2 \beta^3_N, \tag{37}$$

where $f = \ell$, q, the couplings $C_{\ell,\nu,N} = 1$, $C_q = 3$, and $\beta_i = \sqrt{1 - 4m_i^2/M^2_{Z'}}$ is the speed of particle i. Note that the decay width to Majorana particles is of a threshold behavior β^3, and is half of that for a Dirac particle. Well above the threshold, the Z' decay branching fractions take the simple ratios for the final states

$$\sum_\ell^{e,\mu,\tau} \ell^+\ell^- : \sum_q^{u\ldots t} q\bar{q} : \sum_m^{1,2,3} \nu_m \nu_m : N_1 N_1 = 3:2:\frac{3}{2}:\frac{1}{2}. \tag{38}$$

We show in Fig. 10 the results for the case $v_S = 3$ TeV. It scales as

$$\Gamma(\text{tot}) \approx 0.2 g^2_{BL} M_{Z'} < 0.05 \left(\frac{M_{Z'}}{v_S}\right)^2 M_{Z'}. \tag{39}$$

Notice that this Z' has the property that its coupling to quarks is suppressed with respect to the couplings to leptons. As is well-known the Z' in left-right symmetric

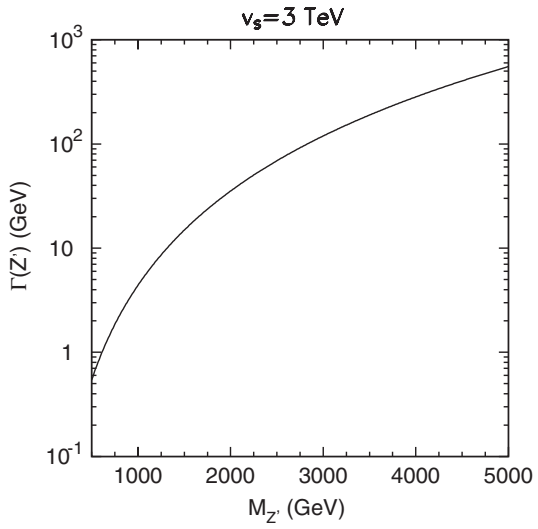

FIG. 10. Total decay width of Z', when $v_S = 3$ TeV.

theories has different properties from the $B-L$ case studied here. Then, from the standard analysis where one uses the leptonic channels and the channels into heavy quarks one can easily distinguish the $B-L$ case from the rest.

It is important to emphasize that in the case of the $B-L$ SM, one gets an upper bound on the mass of the heavy neutrinos $M_N \leq M_{Z'}/(2\sqrt{2}g_{BL})$ (see Appendix C for details).

B. Heavy Majorana neutrino production through Z' mediation at the LHC

We are interested in the production of two heavy neutrinos. Since in this model one has a dynamical mechanism for $B-L$ breaking, there is a production mechanism through the Z'. Then, we are interested in the mechanism

$$pp \to Z' \to N_1 N_1. \tag{40}$$

The parton level cross section for this process is

$$\frac{d\sigma(q\bar{q} \to Z' \to N_1 N_1)}{dt} = \frac{1}{32\pi s^2 N_c}\frac{2g_{BL}^4}{9} \times \frac{1}{(s-M_{Z'}^2)^2 + M_{Z'}^2\Gamma_{Z'}^2} \times [(t-M_N^2)^2 + (u-M_N^2)^2 - 2sM_N^2], \tag{41}$$

where $t=(p_q - p_N)^2$. The total cross section versus heavy Majorana neutrino mass at the LHC is plotted in Fig. 11, assuming $v_S = 3$ TeV with (a) for $U(1)_{B-L}$ coupling and (b) for $U(1)_X$ coupling, as given in Tables I and II. We see that the production cross sections are quite sizable, typically of the order of 10–100 fb. The cross section drops sharply after reaching the kinematical threshold $2M_N > M_{Z'}$.

The Majorana signals for $\Delta L = 2$ decay of N_1 are

$$N_1 N_1 \to \ell^\pm \ell^\pm W^\mp W^\mp, \qquad \ell = e, \mu, \tau. \tag{42}$$

To confirm the important feature of lepton number violation, we demand the W's decay hadronically. The overall branching fraction to be included becomes

$$\mathrm{BR}\,(N_1 N_1 \to \ell^\pm \ell^\pm 4\ \text{jets}) \approx 2 \cdot \left(\frac{1}{4}\right)^2 \cdot \left(\frac{6}{9}\right)^2 = \frac{1}{18}. \tag{43}$$

Note that there are also accompanying clean channels like $\ell^\pm \ell^\mp + 4$ jets, that are not lepton-number violating and we do not include them for the rest of the analysis.

We would like to reiterate that in a significant range of the parameter space of M_N and mixings, the N decay could lead to distinctive signatures with a decay length longer than 10 μm, resulting in secondary displaced vertices. This may yield essentially background-free signal for N's. Nevertheless, we now explore the signal observability according to the different lepton flavors without relying on the displaced vertex considerations.

For our numerical analyses, we adopt the CTEQ6L1 parton distribution function [20]. We evaluate the SM backgrounds by using the automatic package MADGRAPH [21]. We work in the parton level, but simulate the detector effects by the kinematical acceptance and employ the Gaussian smearing for the electromagnetic and hadronic energies [22].

C. $N_1 N_1 \to \ell^\pm \ell^\pm$ + 4 jets ($\ell = e, \mu$)

We start from the cleanest channels with e, μ in the final state from N_1 decay. We employ the following basic acceptance cuts for the event selection [22]

$$p_T(\ell) \geq 15\ \text{GeV}, \qquad |\eta(\ell)| < 2.5, \tag{44}$$

$$p_T(j) \geq 25\ \text{GeV}, \qquad |\eta(j)| < 3.0, \tag{45}$$

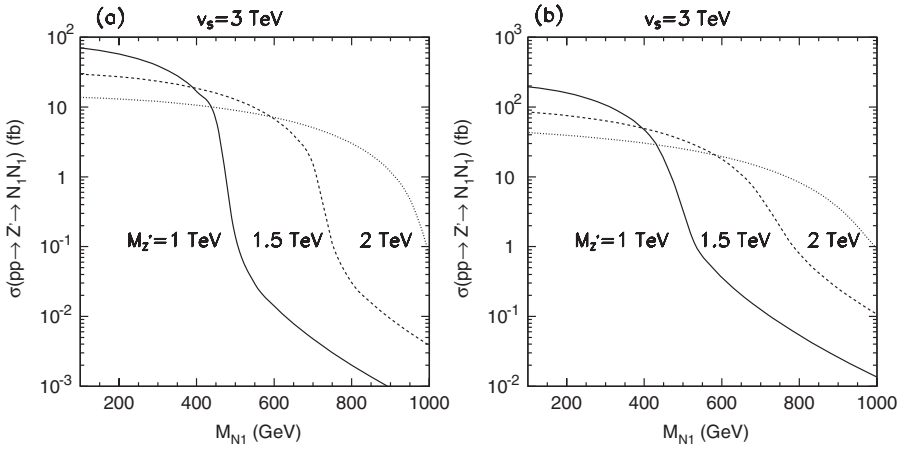

FIG. 11. Heavy Majorana neutrino pair production total cross section at the LHC versus its mass. The solid, dashed, and dotted curves are for $M_{Z'} = 1, 1.5, 2$ TeV, respectively, when $v_S = 3$ TeV, (a) for $U(1)_{B-L}$ coupling and (b) for $U(1)_X$ coupling, as given in Tables I and II.

TABLE I. Feynman rules for Z' and heavy Majorana neutrino N in SM with $U(1)_{B-L}$ extension, where $U^{\nu N} = U^\dagger V$.

Fields	Vertices	Couplings	Approximations
Z'	$\bar{q}_i q_i Z'$	$-iQ^q_{BL} g_{BL}\gamma^\mu$	
	$q_1 = u,\ q_2 = d$	$Q^q_{BL} = \frac{1}{3}$	
	$\bar{\ell}\ell Z'$	$-iQ^\ell_{BL} g_{BL}\gamma^\mu$	
	$\ell = e,\ \mu,\ \tau$	$Q^\ell_{BL} = -1$	
	$\bar{N}_{m_1} N_{m_2} Z'$	$-i(U^T_C U^*_C - V^T V^*)_{m_1 m_2} Q^\ell_{BL} g_{BL}\gamma^\mu \frac{\gamma_5}{2}$	$iI_{m_1 m_2} g_{BL}\gamma^\mu \frac{\gamma_5}{2}$
	$\bar{\nu}_{m_1}\nu_{m_2} Z'$	$-i(U^\dagger U - V^\dagger_C V_C)_{m_1 m_2} Q^\ell_{BL} g_{BL}\gamma^\mu \frac{-\gamma_5}{2}$	$iI_{m_1 m_2} g_{BL}\gamma^\mu \frac{-\gamma_5}{2}$
N_m	$\bar{N}^c_m \ell^- W^+$	$-i\frac{g}{\sqrt{2}} V^*_{\ell m}\gamma^\mu P_L$	
	$N^T_m \ell^- W^+$	$-i\frac{g}{\sqrt{2}} V^*_{\ell m} C\gamma^\mu P_L$	
	$\bar{\nu}_{m_1} N^c_{m'_2} Z$	$-i\frac{g}{2c_W} U^{\nu N}_{m_1 m'_2}\gamma^\mu P_L$	
	$\bar{\nu}_{m_1} \bar{N}^T_{m'_2} Z$	$-i\frac{g}{2c_W} U^{\nu N}_{m_1 m'_2}\gamma^\mu P_L C$	
	$\bar{\nu}_{m_1} N_m h$	$-iV_{\ell m} P_R(\frac{M^N_m}{v_0} c_{\theta 0} + \frac{M^N_m}{v_S} s_{\theta 0})$	$-iV_{\ell m} P_R \frac{M^N_m}{v_0} c_{\theta 0}$
	$\bar{\nu}_\ell N_m H$	$-iV_{\ell m} P_R(\frac{M^N_m}{v_0} s_{\theta 0} + \frac{M^N_m}{v_S} c_{\theta 0})$	$-iV_{\ell m} P_R \frac{M^N_m}{v_0} s_{\theta 0}$

$$\Delta R_{jj} \geq 0.3, \qquad \Delta R_{j\ell}, \qquad \Delta R_{\ell\ell} \geq 0.4. \tag{46}$$

The rather loose cuts on the separations ΔR are designed to keep the signal events for a heavier Z' and a lighter N which is fast moving and thus yields collimated decay products of a lepton and two jets. We plot the minimal isolation $\Delta R^{\min}_{jj}$ of two jets and $\Delta R^{\min}_{\ell j}$ of one jet and one charged lepton for $M_{Z'} = 1$ TeV and $M_N = 100, 200$ GeV, respectively, in Fig. 12. One can see that for $M_N \gtrsim 200$ GeV with $M_{Z'} = 1$ TeV the signal consists of one pair of well-isolated same-sign leptons of arbitrary e, μ flavor combinations plus four light jets.

TABLE II. Feynman rules for Z' in SM with $U(1)_X$ extension, where $s'(c') = \sin(\theta')(\cos(\theta'))$, $\tan(2\theta') = 2g'_1\sqrt{g_2^2 + g_1^2}/(g_1'^2 + 25 g^2_{BL}\frac{v_S^2}{v_0^2} - g_2^2 - g_1^2)$ and all momenta are incoming.

Fields	Vertices	Couplings	Approximations
Z'	$\bar{u}_L u_L Z'$	$iX_{u_L}\gamma^\mu P_L$	
		$X_{u_L} = (1 - \frac{2}{3}s^2_W)s'\sqrt{g_2^2 + g_1^2} + \frac{1}{3}c' g'_1 + \frac{5}{4}Q^q_{BL} c' g_{BL}$	
	$\bar{u}_R u_R Z'$	$iX_{u_R}\gamma^\mu P_R$	
		$X_{u_R} = -\frac{2}{3}s^2_W s'\sqrt{g_2^2 + g_1^2} - \frac{2}{3}c' g'_1 + \frac{5}{4}Q^q_{BL} c' g_{BL}$	
	$\bar{d}_L u_L Z'$	$iX_{d_L}\gamma^\mu P_L$	
		$X_{d_L} = (-\frac{1}{2} + \frac{1}{3}s^2_W)s'\sqrt{g_2^2 + g_1^2} - \frac{1}{6}c' g'_1 + \frac{5}{4}Q^q_{BL} c' g_{BL}$	
	$\bar{d}_R u_R Z'$	$iX_{d_R}\gamma^\mu P_R$	
		$X_{d_R} = \frac{1}{3}s^2_W s'\sqrt{g_2^2 + g_1^2} + \frac{1}{3}c' g'_1 + \frac{5}{4}Q^q_{BL} c' g_{BL}$	
	$\bar{\ell}_L \ell_L Z'$	$iX_{\ell_L}\gamma^\mu P_L$	
		$X_{\ell_L} = (-\frac{1}{2} + s^2_W)s'\sqrt{g_2^2 + g_1^2} + \frac{1}{2}c' g'_1 + \frac{5}{4}Q^q_{BL} c' g_{BL}$	
	$\bar{\ell}_R \ell_R Z'$	$iX_{\ell_R}\gamma^\mu P_R$	
	$\ell = e,\ \mu,\ \tau$	$X_{\ell_R} = s^2_W s'\sqrt{g_2^2 + g_1^2} + c' g'_1 + \frac{5}{4}Q^\ell_{BL} c' g_{BL}$	
	$\bar{N}_{m_1} N_{m_2} Z'$	$i(X^U_N U^T_C U^*_C + X^V_N V^T V^*)_{m_1 m_2}\gamma^\mu \frac{\gamma_5}{2}$	$iX^U_N I_{m_1 m_2}\gamma^\mu \frac{\gamma_5}{2}$
	$\bar{\nu}_{m_1}\nu_{m_2} Z'$	$i(X^U_\nu U^\dagger U + X^V_\nu V^\dagger_C V_C)_{m_1 m_2}\gamma^\mu \frac{-\gamma_5}{2}$	$iX^U_\nu I_{m_1 m_2}\gamma^\mu \frac{-\gamma_5}{2}$
		$X^U_N = -X^V_\nu = \frac{5}{4}Q^\ell_{BL} c' g_{BL}$	
		$X^U_\nu = -X^V_N = \frac{1}{2}s'\sqrt{g_2^2 + g_1^2} + \frac{1}{2}c' g'_1 + \frac{5}{4}Q^\ell_{BL} c' g_{BL}$	
	$W^-_\mu(p_1) W^+_\nu(p_2) Z'_\rho(p_3)$	$-ig c_W s'[(p_1 - p_2)_\rho g_{\mu\nu} + (p_2 - p_3)_\mu g_{\nu\rho} + (p_3 - p_1)_\nu g_{\rho\mu}]$	
	$hZ_\mu Z'_\nu$	$2i[v_0\frac{c_{\theta 0}}{4}K - v_S s_{\theta 0} K']g_{\mu\nu}$	
	$HZ_\mu Z'_\nu$	$2i[v_0\frac{s_{\theta 0}}{4}K + v_S c_{\theta 0} K']g_{\mu\nu}$	
		$K = -\sin(2\theta')(g_1^2 + g_2^2 + g_1'^2) - 2\cos(2\theta')g'_1\sqrt{g_1^2 + g_2^2}$	
		$K' = \frac{25}{4}\sin(2\theta')g^2_{BL}$	

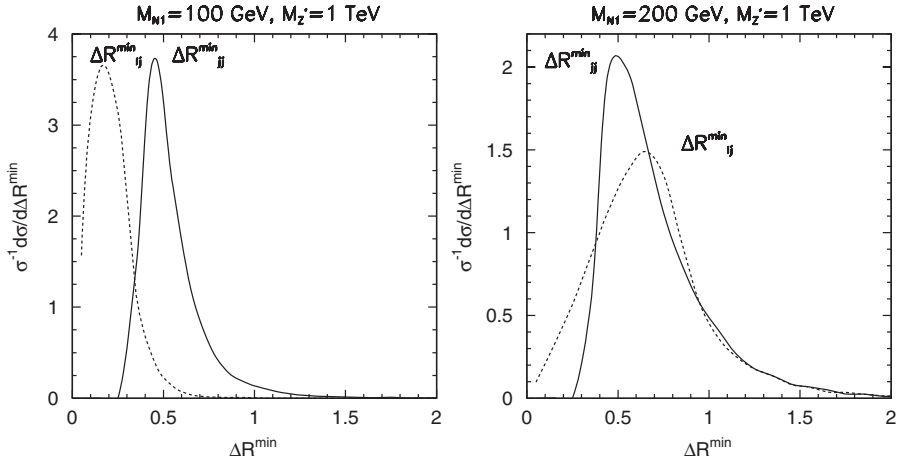

FIG. 12. $\Delta R_{jj}^{\min}$ and $\Delta R_{\ell j}^{\min}$ for $M_{N_1} = 100$ GeV (left) and $M_{N_1} = 200$ GeV (right), with $M_{Z'} = 1$ TeV.

To simulate the detector effects on the energy-momentum measurements, we smear the electromagnetic energy and jet energy by a Gaussian distribution whose width is parametrized as [22]

$$\frac{\Delta E}{E} = \frac{a_{\rm cal}}{\sqrt{E/\text{GeV}}} \oplus b_{\rm cal}, \qquad a_{\rm cal} = 10\%, \qquad b_{\rm cal} = 0.7\%, \tag{47}$$

$$\frac{\Delta E}{E} = \frac{a_{\rm had}}{\sqrt{E/\text{GeV}}} \oplus b_{\rm had}, \qquad a_{\rm had} = 50\%, \qquad b_{\rm had} = 3\%. \tag{48}$$

In principle, there is no genuine SM background to the lepton-number violating processes. The leading SM background to our signal is from decays of two like-sign W's to leptons. For instance, the leading reducible background to our signal is

$$pp \to t\bar{t}W^{\pm} \to W^{\pm}W^{\pm}jjb\bar{b}. \tag{49}$$

The QCD processes $jjjjW^{\pm}W^{\pm}$, $jjW^{\pm}W^{\pm}W^{\mp}$ are much smaller. This is estimated based on the fact that QCD $jjW^{\pm}W^{\pm} \to jj\ell^{\pm}\ell^{\pm}\not{E}_T$ is about 15 fb. With an additional α_s^2 and 6-body phase space or one more W suppression, they are much smaller than $t\bar{t}W^{\pm}$. Other electroweak backgrounds $WWWW$, $WWWZ$ are also neglectable. Although the background rates are large to begin with, the kinematics is quite different between the signal and the backgrounds. We outline the characteristics and propose some judicious cuts as follows.

(i) The SM backgrounds always come with W pair decays with missing neutrinos. To suppress backgrounds, we veto the events with large missing energy $\not{E}_T < 20$ GeV.

(ii) We choose the two pairs with nearly equal masses from the six dijet combinations as the two hadronic W's and take W boson reconstruction as $|M_{jj} - M_W| < 15$ GeV. The efficiency is very high.

(iii) In order to select the correct lepton and two jets combination and reconstruct N_1, we take advantage of the feature that the two heavy neutrinos have equal masses $M_{\ell_1 j_1 j_2} = M_{\ell_2 j_3 j_4}$. In practice, we impose $|M_{\ell_1 j_1 j_2} - M_{\ell_2 j_3 j_4}| < M_{N_1}/25$. This helps for the background reduction.

The production cross section of N_1N_1 signal with the basic cuts (solid curve) and all of the cuts above (dashed curve) are plotted in Fig. 13, where branching fractions for N_1 decay to charged leptons are not included; while W decays to two jets are included. For comparison, the background process of $t\bar{t}W^{\pm}$ is also included with the sequential cuts as indicated. The background is suppressed substantially.

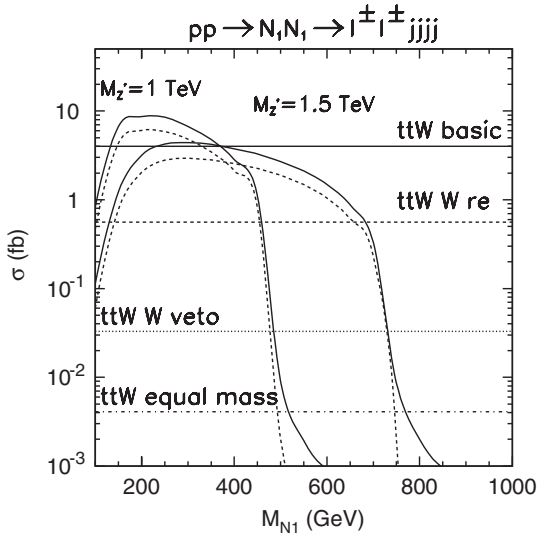

FIG. 13. Production cross section of N_1N_1 with basic cuts and hard final states cuts. Branching fractions for N_1 decay to charged leptons are not included; while W decays to two jets are included. For comparison, the background process is also included with the sequential cuts as indicated.

When performing the signal significance analysis, we look for the resonance in the mass distributions of ℓjj and $2\ell 4j$. If we look at mass window of $|M_{\ell_1 j_1 j_2, \ell_2 j_3 j_4} - M_{N_1}| < M_{N_1}/20$ and $|M_{2\ell+4j} - M_{Z'}| < M_{Z'}/30$, the background will be at a negligible level.

D. $N_1 N_1 \to \tau^\pm \ell^\pm + 4$ jets

The previous section sets the stage for the analyses in the following sections. Most of the issues for event selection and detector acceptance will remain the same for the following studies. The next presentations will thus be sketchy and mainly outlining the new features, in particular, the τ reconstruction and the mass resonances.

The τ lepton final state from heavy Majorana neutrino decay plays an important role in distinguishing different neutrino mass patterns. Its identification and reconstruction are different from e, μ final states because a τ decays promptly and there will always be missing neutrinos in τ decay products. In practice when selecting events with τ's, we require a minimal missing transverse energy

$$\not{E}_T > 20 \text{ GeV}. \tag{50}$$

This will effectively separate them from the $\ell\ell jjjj$ type of signal events.

We first note that all the τ's are very energetic from the decay of a few hundred GeV N_1. The missing momentum will be along the direction of the charged track. We thus assume the momentum of the missing neutrinos to be reconstructed by

$$\vec{p}(\text{invisible}) = \kappa \vec{p}(\text{track}). \tag{51}$$

Identifying $\vec{p}_T(\text{invisible})$ with the measured $\not{E}_T$, we thus obtain the τ momentum by

$$\vec{p}_T(\tau) = \vec{p}_T(\ell) + \vec{\not{E}}_T, \qquad p_L(\tau) = p_L(\ell) + \frac{\not{E}_T}{p_T(\ell)} p_L(\ell).$$

The N_1 pair kinematics is thus fully reconstructed. The reconstructed invariant masses of $M(\ell jj)$ and $M(\tau jj)$ are plotted in Fig. 14. We see that $M(\tau jj)$ distribution (dotted curve) is slightly broader as anticipated. The rather narrow mass peak of the ℓjj system nevertheless serves as the most distinctive kinematical feature for the signal identification. Invariant masses of $M(\tau\ell + 4j)$ are also plotted in Fig. 14. Although the existence of missing energy in the signal makes the background separation more involved, the resonant mass reconstruction proves to be highly efficient and the backgrounds can still be suppressed to a negligible level.

E. $N_1 N_1 \to \tau^\pm \tau^\pm + 4$ jets

For $\tau\tau jjjj$ events with two τ's, we generalize the momenta reconstruction to

$$\vec{p}(\text{invisible}) = \kappa_1 \vec{p}(\text{track}_1) + \kappa_2 \vec{p}(\text{track}_2). \tag{52}$$

The proportionality constants κ_1, κ_2 can be determined from the missing energy measurement as long as the two charge tracks are linearly independent. The N_1 pair kinematics can be once again fully reconstructed. The reconstructed invariant masses of $M(\tau jj)$ are plotted in Fig. 15. The nice mass peaks of the τjj system at M_{N_1} and the $\tau\tau jj$ system at $M_{Z'}$ make the signal stand out of the SM backgrounds.

It is important to note a difference between the leptons from the primary N_1 decay and from the τ decay: the latter is much softer. In Fig. 16 we show the p_T distribution of the softer lepton from the N_1 and τ decays in the events of $\ell\ell jjjj$, $\ell\tau jjjj$ and $\tau\tau jjjj$. This feature could provide additional discrimination power to separate the three different leptonic channels if needed to fit the flavor structure for an underlying theory.

F. Measuring branching fractions and probing the neutrino mass patterns

So far, we have only studied the characteristic features of the signal and backgrounds for the leading channels and have not included the proper branching fractions for the

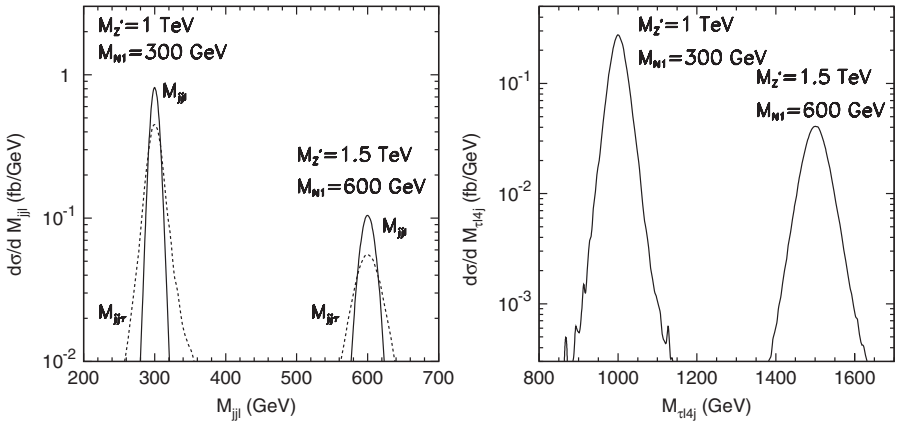

FIG. 14. Reconstructed invariant mass of $M(jj\ell)$, $M(jj\tau)$ for $M_{N_1} = 300, 600$ GeV, respectively, (left) and $M(\tau\ell 4j)$ for $M_{Z'} = 1, 1.5$ TeV (right).

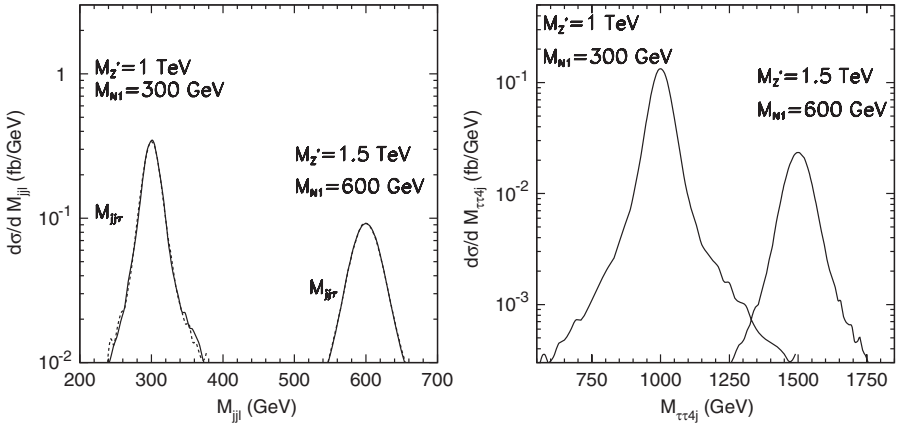

FIG. 15. Reconstructed invariant mass of $M(jj\tau)$ for $M_{N_1} = 300, 600$ GeV, respectively, (left) and $M(\tau\tau 4j)$ for $M_{Z'} = 1, 1.5$ TeV (right).

individual lepton flavors. For illustration, consider first the cleanest channel, $N_1N_1 \to e^\pm e^\pm jjjj$. The number of events is written as

$$N = L \times \sigma(pp \to N_1N_1) \times 2\ \mathrm{BR}^2(N_1 \to e^+W^-)\left(\frac{6}{9}\right)^2, \tag{53}$$

where L is the integrated luminosity and the factor $(6/9)$ is due to the W hadronic decay. Given a sufficient number of events N, the mass of N_1 is determined by the invariant mass of lepton and jet $M_{\ell jj}$. We thus predict the corresponding production rate $\sigma(pp \to N_1N_1)$ for this given mass. The only unknown in Eq. (53) is the decay branching fraction.

We present the event contours in the BR $- M_N$ plane (where BR is the branching ratio) in Fig. 17 for 100 fb^{-1} luminosity and degenerate case with (a) $M_{Z'} = 1$ TeV and (b) $M_{Z'} = 1.5$ TeV including all the judicious cuts described earlier, with which the backgrounds are insignificant.

In Figs. 17(c) and 17(d), we show the event contours in the BR $- M_{N_1}$ plane, for 100 fb^{-1} luminosity and nondegenerate case including all the judicious cuts described earlier. We see that the reach to a low BR can be quite encouraging.

As we presented earlier, the N_1 decay branching fractions and the light neutrino mass matrix are directly correlated. Measuring the BR's of different flavor combinations becomes crucial in understanding the neutrino mass pattern and thus the mass generation mechanism. In the degenerate case, we have the prediction for the flavor combinations

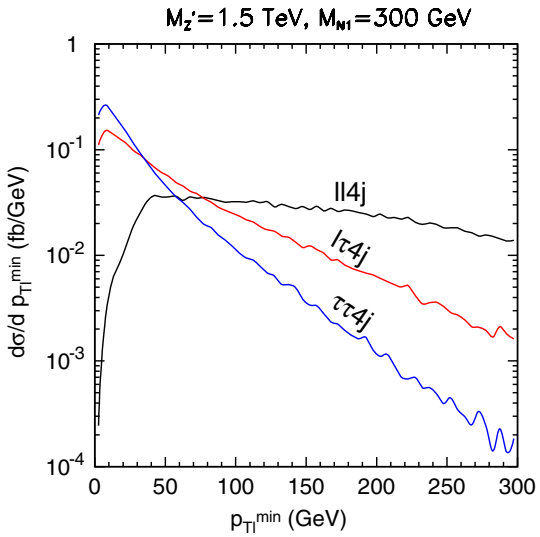

FIG. 16 (color online). p_T distribution of the softer lepton from the N_1 and τ decays in the events of $\ell\ell jjjj$, $\ell\tau jjjj$ and $\tau\tau jjjj$, for a N_1 mass 300 GeV and Z' mass 1.5 TeV.

$$\mathrm{BR}\,(NN \to \ell\ell WW) \approx \begin{cases} 2\times(23\%)^2 \text{ for NH:} (\mu^\pm + \tau^\pm)(\mu^\pm + \tau^\pm)WW, \\ 2\times(13\%)^2 \text{ for IH:} e^\pm e^\pm WW, \\ 2\times(17\%)^2 \text{ for QD:} (e^\pm + \mu^\pm + \tau^\pm)(e^\pm + \mu^\pm + \tau^\pm)WW, \end{cases} \tag{54}$$

for $\Phi_1 = \Phi_2 = 0$, independent of the matrix Ω. On the other hand, for the nondegenerate situation, the flavor prediction is like

$$\mathrm{BR}\,(NN \to \ell\ell WW) \approx \begin{cases} 2 \times (20\%)^2 & \text{for } \mathrm{N}_1\text{: } e^\pm e^\pm WW, \\ 2 \times (17\%)^2 & \text{for } \mathrm{N}_2\text{: } (e^\pm + \mu^\pm + \tau^\pm)(e^\pm + \mu^\pm + \tau^\pm)WW, \\ 2 \times (23\%)^2 & \text{for } \mathrm{N}_3\text{: } (\mu^\pm + \tau^\pm)(\mu^\pm + \tau^\pm)WW, \end{cases} \tag{55}$$

for $\Omega = I$, independent of the neutrino mass patterns as well as Φ_1, Φ_2. These predictions are the consequence from the

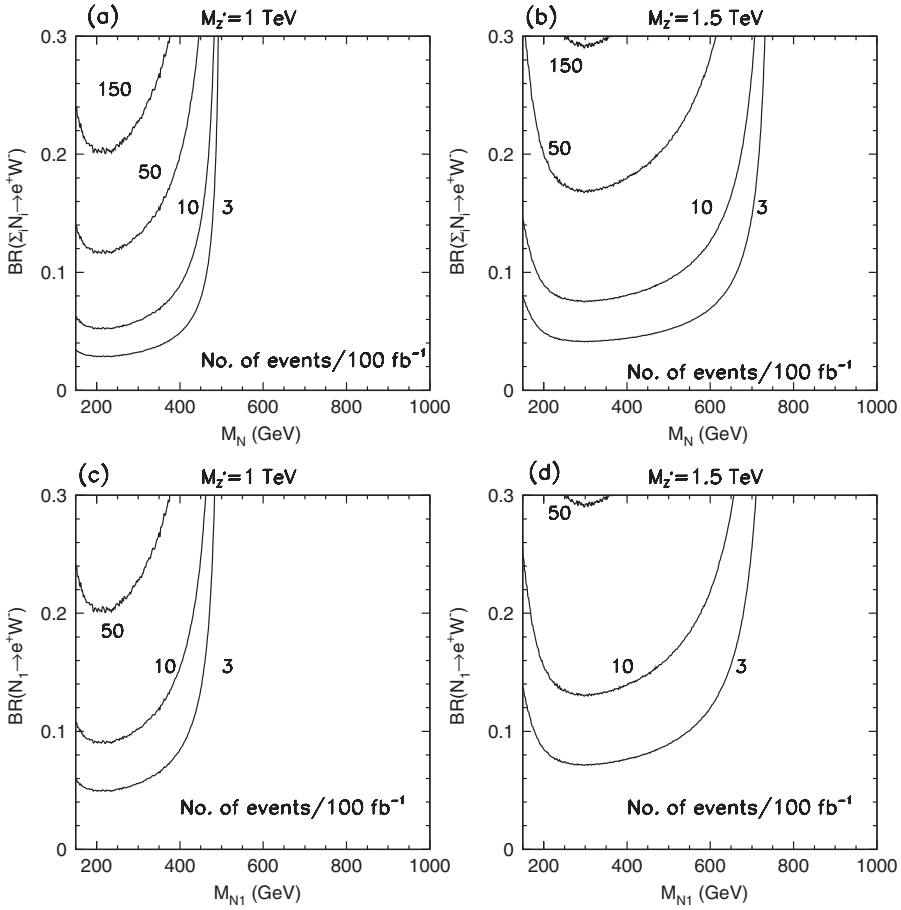

FIG. 17. Event contours in the BR $-$ M_N plane at the LHC with an integrated luminosity 100 fb^{-1} for degenerate case $\sum_{i=1,2,3} N_i N_i \to e^+ e^+ W^- W^-$ with (a) $M_{Z'} = 1$ TeV, (b) $M_{Z'} = 1.5$ TeV, and for nondegenerate case $N_1 N_1 \to e^+ e^+ W^- W^-$ with (c) $M_{Z'} = 1$ TeV and (d) $M_{Z'} = 1.5$ TeV, including all the judicious cuts described in the early sections.

low energy oscillation experiments and this are subject to test at the LHC to confirm the theory.

In Fig. 18 we show the event contours in the $M_{Z'} - M_N$ plane, for (a) production of $\sum_i N_i$ in NH (solid curve), IH

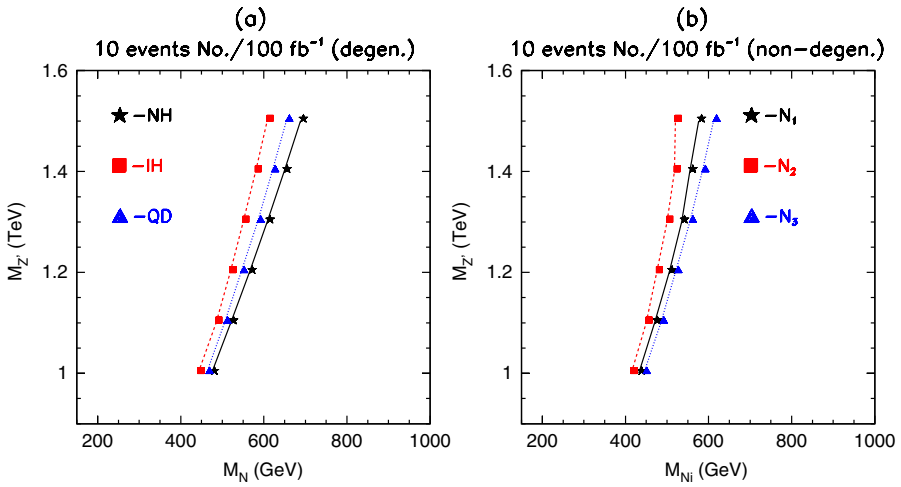

FIG. 18 (color online). Event contours in the $M_{Z'} - M_N$ plane at the LHC with an integrated luminosity 100 fb^{-1} and 10 event numbers for (a) degenerate case $\sum_{i=1,2,3} N_i N_i \to \ell^\pm \ell^\pm W W$ for NH, IH, and QD, and (b) nondegenerate case for N_1, N_2, and N_3, all as predicted in Eqs. (54) and (55).

(dashed curve), and QD (dotted curve) for the degenerate case and (b) production of N_1 (solid curve), N_2 (dashed curve), and N_3 (dotted curve) for the nondegenerate case with 100 fb^{-1} luminosity, 10 event numbers, and branching fractions of heavy neutrinos predicted in Eqs. (54) and (55). The values of $M_{Z'}$ and M_N on the left-hand side of the curves would give more than 10 events for 100 fb^{-1} luminosity and more accessible heavy neutrino decay branching fractions at the LHC.

V. SUMMARY

In this article we have investigated the possibility to test the so-called type I seesaw mechanism for neutrino masses at the CERN Large Hadron Collider in the context of two simple extensions of the standard model where $B - L$ is part of the gauge symmetry. We have studied in great detail the predictions of the right-handed neutrino decays in each spectrum for neutrino masses showing the most optimistic scenarios where one could hope to distinguish the spectrum using the properties of the decays.

We have found the following interesting results:

(i) Working in the context of two simple extensions of the standard model with a local gauge symmetry $B - L$ or $X = Y - \frac{5}{4}(B - L)$, one can produce the heavy neutrinos through the Z' gauge boson in each scenario. In both cases one has a dynamical mechanism for the generation of heavy neutrino masses, related to $M_{Z'}$.

(ii) In the case where the heavy neutrinos are degenerate, we show the possibility to distinguish the neutrino spectrum. The branching fractions can differ by 1 order of magnitude in NH case with $\mathrm{BR}(\mu^{\pm}W^{\mp})$, $\mathrm{BR}(\tau^{\pm}W^{\mp}) \gg \mathrm{BR}(e^{\pm}W^{\mp})$, and a factor of a few in the IH spectrum with $\mathrm{BR}(e^{\pm}W^{\mp}) > \mathrm{BR}(\mu^{\pm}W^{\mp})$, $\mathrm{BR}(\tau^{\pm}W^{\mp})$ when the Majorana phases are ignored. As one expects, all these channels are quite similar when the neutrino spectrum is quasidegenerate, $m_1 \approx m_2 \approx m_3 \geq 0.05$ eV.

(iii) In the case when Ω is an identity matrix or with only unity entries generally, we find: $\mathrm{BR}(e^{\pm}W^{\mp}) > \mathrm{BR}(\mu^{\pm}W^{\mp})$, $\mathrm{BR}(\tau^{\pm}W^{\mp})$ for N_1 decay, $\mathrm{BR}(e^{\pm}W^{\mp}) \approx \mathrm{BR}(\mu^{\pm}W^{\mp}) \approx \mathrm{BR}(\tau^{\pm}W^{\mp})$ for N_2, and $\mathrm{BR}(\mu^{\pm}W^{\mp})$, $\mathrm{BR}(\tau^{\pm}W^{\mp}) \gg \mathrm{BR}(e^{\pm}W^{\mp})$ for N_3 in both NH and IH. The branching fractions in these cases are independent of Majorana phases.

(iv) In general, the form of Ω governs heavy neutrino decay patterns. Future tests on the flavor combinations of SM charged leptons would reveal the specific model structure.

(v) The above-studied $\Delta L = 2$ channels can take the search to $M_{Z'} \approx 2$ TeV at the LHC. The sensitivity to the leptonic branching fractions of N decay can be about 10%.

(vi) In particular, in a significant part of the parameter space of M_N and the mixings, the N decay could lead to distinctive signatures with secondary displaced vertices. yielding essentially background-free signal for N's.

ACKNOWLEDGMENTS

The work of P. F. P. was supported in part by the U.S. Department of Energy Contract No. DE-FG02-08ER41531 and in part by the Wisconsin Alumni Research Foundation. The work of T. H. is supported in part by the U.S. Department of Energy under Grant No. DE-FG02-95ER40896, and by the Wisconsin Alumni Research Foundation. T. L. would like to thank Xiao-Gang He for helpful discussions. P. F. P. would like to thank S. Blanchet for discussions.

APPENDIX A: NEUTRINO MASSES AND MIXINGS

The type I seesaw scheme introduces right-handed neutrino states, in addition to the SM matter contents. For definitiveness, we add three of them, ν_R^i $(i = 1, 2, 3)$, which are said to be sterile since they do not carry any SM gauge quantum numbers. The SM gauge invariant and renormalizable interactions to generate neutrino masses include both Dirac as well as Majorana terms

$$-\mathcal{L}_\nu^I = \bar{l}_L Y_\nu^D \tilde{H} \nu_R + \frac{1}{2}(\bar{\nu}^c)_L M_N \nu_R + \text{H.c.}, \tag{A1}$$

where Y_ν^D, M_N are 3×3 matrices in the generation space, with $\tilde{H} = i\sigma_2 H^*$ and $H^T = (H^+ H^0)$. Once H gets the vacuum expectation value $\langle H \rangle = v_0/\sqrt{2}$, the neutrinos acquire Dirac masses $m_D = Y_\nu^D v_0/\sqrt{2}$,

$$-\mathcal{L}_\nu^m = \frac{1}{2}(\bar{\nu}_L m_D \nu_R + (\bar{\nu}^c)_L m_D^T (\nu^c)_R + (\bar{\nu}^c)_L M_N \nu_R) + \text{H.c.} \tag{A2}$$

To diagonalize the mass matrix for neutrinos we introduce a 6×6 unitary transformation

$$\begin{pmatrix} \nu_L \\ (\nu^c)_L \end{pmatrix} = \mathbb{N} \begin{pmatrix} \nu_L \\ (\nu^c)_L \end{pmatrix}_{\text{mass}}, \qquad \mathbb{N} = \begin{pmatrix} U & V \\ V_C & U_C \end{pmatrix}. \tag{A3}$$

Then,

$$\mathbb{N}^\dagger \begin{pmatrix} 0 & m_D \\ m_D^T & M_N \end{pmatrix} \mathbb{N}^* = \begin{pmatrix} m & 0 \\ 0 & M \end{pmatrix}, \tag{A4}$$

or explicitly,

$$V_C^\dagger m_D^T U^* + U^\dagger m_D V_C^* + V_C^\dagger M_N V_C^* = m, \tag{A5}$$

$$U_C^\dagger m_D^T V^* + V^\dagger m_D U_C^* + U_C^\dagger M_N U_C^* = M, \tag{A6}$$

$$V_C^\dagger m_D^T V^* + U^\dagger m_D U_C^* + V_C^\dagger M_N U_C^* = 0, \tag{A7}$$

where $m = \mathrm{diag}(m_1, m_2, m_3)$ and $M = \mathrm{diag}(M_1, M_2, M_3)$ are diagonal matrices of the mass eigenvalues. In the limit $M_N \gg m_D$ we have

$$m \approx \frac{m_D^2}{M_N}, \qquad M \approx M_N. \tag{A8}$$

Then we have three light neutrinos and three heavy ones, all Majorana-type. Note that U and V mix the light and heavy neutrinos, respectively, into the active weak interaction eigenstates of neutrinos. The mixing elements are typically like

$$U^2 \approx \mathcal{O}(1), \qquad V^2 \approx \frac{m}{M}, \tag{A9}$$

and the unitarity conditions read

$$\begin{aligned} UU^\dagger + VV^\dagger &= U^\dagger U + V_C^\dagger V_C = V_C V_C^\dagger + U_C U_C^\dagger \\ &= V^\dagger V + U_C^\dagger U_C = I, \end{aligned} \tag{A10}$$

$$UV_C^\dagger + VU_C^\dagger = U^\dagger V + V_C^\dagger U_C = 0. \tag{A11}$$

It can be shown that the following relations hold:

$$V_C^\dagger m_D^T - mU^T = 0, \qquad m_D U_C^* - VM = 0. \tag{A12}$$

Assuming that a 3×3 matrix E diagonalizes the mass matrix of the charged leptons, we then define

$$E^\dagger U \equiv V_{\rm PMNS}, \qquad E^\dagger V \equiv V_{\ell N}, \tag{A13}$$

$$V_{\rm PMNS} V_{\rm PMNS}^\dagger + V_{\ell N} V_{\ell N}^\dagger = I, \tag{A14}$$

where $V_{\rm PMNS}$ and $V_{\ell N}$ describe the transitions between the light neutrino and heavy neutrino to the charged leptons, respectively, via the weak charged currents. Note that the identification of $V_{\rm PMNS}$ to the PMNS matrix is only approximate. We then obtain an important relation among the physical quantities

$$V_{\ell N}^* M V_{\ell N}^\dagger = -V_{\rm PMNS}^* m V_{\rm PMNS}^\dagger. \tag{A15}$$

Although the masses and mixings of the light neutrinos on the right-handed side can be measured from the oscillation experiments, it is quite involved to solve for $V_{\ell N}$ via this set of quadratic equations. Absorbing the minus sign on the right side of the above equation in the definition of $V_{\ell N}$ one can write down a formal solution with the help of an auxiliary matrix

$$V_{\ell N} = V_{\rm PMNS} m^{1/2} \Omega M^{-1/2}, \tag{A16}$$

where Ω is an orthogonal complex matrix which can be parametrized as

$$\Omega(w_{21}, w_{31}, w_{32}) = R_{12}(w_{21}) R_{13}(w_{31}) R_{23}(w_{32}), \tag{A17}$$

with

$$\begin{aligned} R_{12} &= \begin{pmatrix} u_{21} & -w_{21} & 0 \\ w_{21} & u_{21} & 0 \\ 0 & 0 & 1 \end{pmatrix}, \\ R_{13} &= \begin{pmatrix} u_{31} & 0 & -w_{31} \\ 0 & 1 & 0 \\ w_{31} & 0 & u_{31} \end{pmatrix}, \\ R_{23} &= \begin{pmatrix} 1 & 0 & 0 \\ 0 & u_{32} & -w_{32} \\ 0 & w_{32} & u_{32} \end{pmatrix}, \end{aligned} \tag{A18}$$

where $u_{ij} = \pm\sqrt{1 - w_{ij}^2}$ and $-1 \le w_{ij} \le 1$ when the matrix Ω is real.

APPENDIX B: EXPLICIT EXPRESSIONS FOR THE MIXINGS $V_{\ell N}$

1. Case I: Degenerate heavy neutrinos

From Eq. (A15), assuming degenerate heavy neutrinos, we have

$$\begin{aligned} M_N \sum_N (V_{eN}^*)^2 &= c_{13}^2 s_{12}^2 m_2 + c_{12}^2 c_{13}^2 e^{-i\Phi_1} m_1 \\ &\quad + s_{13}^2 e^{i(2\delta - \Phi_2)} m_3, \end{aligned} \tag{B1}$$

$$\begin{aligned} M_N \sum_N (V_{\mu N}^*)^2 &= (c_{12}c_{23} - s_{12}s_{13}s_{23}e^{-i\delta})^2 m_2 \\ &\quad + (c_{23}s_{12} + c_{12}s_{13}s_{23}e^{-i\delta})^2 e^{-i\Phi_1} m_1 \\ &\quad + c_{13}^2 s_{23}^2 e^{-i\Phi_2} m_3, \end{aligned} \tag{B2}$$

$$\begin{aligned} M_N \sum_N (V_{\tau N}^*)^2 &= (c_{12}s_{23} + c_{23}s_{12}s_{13}e^{-i\delta})^2 m_2 \\ &\quad + (s_{12}s_{23} - c_{12}c_{23}s_{13}e^{-i\delta})^2 e^{-i\Phi_1} m_1 \\ &\quad + c_{13}^2 c_{23}^2 e^{-i\Phi_2} m_3. \end{aligned} \tag{B3}$$

2. Case II: Nondegenerate heavy neutrinos

The general expressions for the mixing between the charged leptons and heavy neutrinos, in terms of the neutrino oscillation parameters and the unknown matrix Ω, are given by

$$\begin{aligned} V_{e1}\sqrt{M_1} &= \sqrt{m_2} c_{13} s_{12} w_{21} \sqrt{1 - w_{31}^2} \\ &\quad + \sqrt{m_1} c_{12} c_{13} \sqrt{(1 - w_{21}^2)(1 - w_{31}^2)} e^{i\Phi_1/2} \\ &\quad + \sqrt{m_3} s_{13} w_{31} e^{i(\Phi_2/2 - \delta)}, \end{aligned} \tag{B4}$$

$$V_{\mu 1}\sqrt{M_1} = \sqrt{m_2}(c_{12}c_{23} - s_{12}s_{13}s_{23}e^{i\delta})w_{21}\sqrt{1-w_{31}^2} + \sqrt{m_1}(-s_{12}c_{23} - c_{12}s_{13}s_{23}e^{i\delta}) \times \sqrt{(1-w_{21}^2)(1-w_{31}^2)}e^{i\Phi_1/2} + \sqrt{m_3}c_{13}s_{23}w_{31}e^{i\Phi_2/2}, \quad \text{(B5)}$$

$$V_{\tau 1}\sqrt{M_1} = \sqrt{m_2}(-c_{12}s_{23} - s_{12}s_{13}c_{23}e^{i\delta})w_{21}\sqrt{1-w_{31}^2} + \sqrt{m_1}(s_{12}s_{23} - c_{12}s_{13}c_{23}e^{i\delta}) \times \sqrt{(1-w_{21}^2)(1-w_{31}^2)}e^{i\Phi_1/2} + \sqrt{m_3}c_{13}c_{23}w_{31}e^{i\Phi_2/2}. \quad \text{(B6)}$$

$$V_{e2}\sqrt{M_2} = \sqrt{m_2}c_{13}s_{12}(-w_{21}w_{31}w_{32} + \sqrt{(1-w_{21}^2)(1-w_{32}^2)}) + \sqrt{m_1}c_{12}c_{13}(-w_{31}w_{32}\sqrt{1-w_{21}^2} - w_{21}\sqrt{1-w_{32}^2})e^{i\Phi_1/2} + \sqrt{m_3}s_{13}w_{32}\sqrt{1-w_{31}^2}e^{i(\Phi_2/2-\delta)}, \quad \text{(B7)}$$

$$V_{\mu 2}\sqrt{M_2} = \sqrt{m_2}(c_{12}c_{23} - s_{12}s_{13}s_{23}e^{i\delta}) \times (-w_{21}w_{31}w_{32} + \sqrt{(1-w_{21}^2)(1-w_{32}^2)}) + \sqrt{m_1}(-s_{12}c_{23} - c_{12}s_{13}s_{23}e^{i\delta}) \times (-w_{32}w_{31}\sqrt{1-w_{21}^2} - w_{21}\sqrt{1-w_{32}^2})e^{i\Phi_1/2} + \sqrt{m_3}c_{13}s_{23}w_{32}\sqrt{1-w_{31}^2}e^{i\Phi_2/2}, \quad \text{(B8)}$$

$$V_{\tau 2}\sqrt{M_2} = \sqrt{m_2}(-c_{12}s_{23} - s_{12}s_{13}c_{23}e^{i\delta}) \times (-w_{21}w_{31}w_{32} + \sqrt{(1-w_{21}^2)(1-w_{32}^2)}) + \sqrt{m_1}(s_{12}s_{23} - c_{12}s_{13}c_{23}e^{i\delta}) \times (-w_{32}w_{31}\sqrt{1-w_{21}^2} - w_{21}\sqrt{1-w_{32}^2})e^{i\Phi_1/2} + \sqrt{m_3}c_{13}c_{23}w_{32}\sqrt{1-w_{31}^2}e^{i\Phi_2/2}. \quad \text{(B9)}$$

$$V_{e3}\sqrt{M_3} = \sqrt{m_2}c_{13}s_{12}(-w_{32}\sqrt{1-w_{21}^2} - w_{21}w_{31}\sqrt{1-w_{32}^2}) + \sqrt{m_1}c_{12}c_{13}(w_{21}w_{32} - w_{31} \times \sqrt{(1-w_{21}^2)(1-w_{32}^2)})e^{i\Phi_1/2} + \sqrt{m_3}s_{13}\sqrt{(1-w_{31}^2)(1-w_{32}^2)}e^{i(\Phi_2/2-\delta)}, \quad \text{(B10)}$$

$$V_{\mu 3}\sqrt{M_3} = \sqrt{m_2}(c_{12}c_{23} - s_{12}s_{13}s_{23}e^{i\delta}) \times (-w_{32}\sqrt{1-w_{21}^2} - w_{21}w_{31}\sqrt{1-w_{32}^2}) + \sqrt{m_1}(-s_{12}c_{23} - c_{12}s_{13}s_{23}e^{i\delta}) \times (w_{32}w_{21} - w_{31}\sqrt{(1-w_{21}^2)(1-w_{32}^2)})e^{i\Phi_1/2} + \sqrt{m_3}c_{13}s_{23}\sqrt{(1-w_{31}^2)(1-w_{32}^2)}e^{i\Phi_2/2}, \quad \text{(B11)}$$

$$V_{\tau 3}\sqrt{M_3} = \sqrt{m_2}(-c_{12}s_{23} - s_{12}s_{13}c_{23}e^{i\delta}) \times (-w_{32}\sqrt{1-w_{21}^2} - w_{21}w_{31}\sqrt{1-w_{32}^2}) + \sqrt{m_1}(s_{12}s_{23} - c_{12}s_{13}c_{23}e^{i\delta}) \times (w_{32}w_{21} - w_{31}\sqrt{(1-w_{21}^2)(1-w_{32}^2)})e^{i\Phi_1/2} + \sqrt{m_3}c_{13}c_{23}\sqrt{(1-w_{31}^2)(1-w_{32}^2)}e^{i\Phi_2/2}. \quad \text{(B12)}$$

We now present the two cases according to the light neutrino mass spectra, assuming $m_{1(3)} \approx 0$ and $s_{13} = 0$.

(i) *Normal hierarchy.*—Under the good approximations $m_1 \approx 0$ and $s_{13} = 0$, one finds the following expressions:

$$M_1|V_{e1}|^2 \approx \sqrt{\Delta m_{21}^2}(s_{12}w_{21}\sqrt{1-w_{31}^2})^2, \quad \text{(B13)}$$

$$M_1|V_{\mu 1}|^2 \approx |\sqrt[4]{\Delta m_{21}^2}c_{12}c_{23}w_{21}\sqrt{1-w_{31}^2} + \sqrt[4]{\Delta m_{31}^2}s_{23}w_{31}e^{i\Phi_2/2}|^2, \quad \text{(B14)}$$

$$M_1|V_{\tau 1}|^2 \approx |\sqrt[4]{\Delta m_{21}^2}c_{12}s_{23}w_{21}\sqrt{1-w_{31}^2} - \sqrt[4]{\Delta m_{31}^2}s_{23}w_{31}e^{i\Phi_2/2}|^2. \quad \text{(B15)}$$

$$M_2|V_{e2}|^2 \approx \sqrt{\Delta m_{21}^2}s_{12}^2(-w_{21}w_{31}w_{32} + \sqrt{(1-w_{21}^2)(1-w_{32}^2)})^2, \quad \text{(B16)}$$

$$M_2|V_{\mu 2}|^2 \approx |\sqrt[4]{\Delta m_{21}^2}c_{12}c_{23}(-w_{21}w_{31}w_{32} + \sqrt{(1-w_{21}^2)(1-w_{32}^2)}) + \sqrt[4]{\Delta m_{31}^2}s_{23}w_{32}\sqrt{1-w_{31}^2}e^{i\Phi_2/2}|^2, \quad \text{(B17)}$$

$$M_2|V_{\tau 2}|^2 \approx |\sqrt[4]{\Delta m^2_{21}}c_{12}s_{23}(-w_{21}w_{31}w_{32} + \sqrt{(1-w^2_{21})(1-w^2_{32})}) - \sqrt[4]{\Delta m^2_{31}}c_{23}w_{32}\sqrt{1-w^2_{31}}e^{i\Phi_2/2}|^2. \quad \text{(B18)}$$

$$M_3|V_{e3}|^2 \approx \sqrt{\Delta m^2_{21}}s^2_{12}(-w_{32}\sqrt{1-w^2_{21}} - w_{21}w_{31}\sqrt{1-w^2_{32}})^2, \quad \text{(B19)}$$

$$M_3|V_{\mu 3}|^2 \approx |\sqrt[4]{\Delta m^2_{21}}c_{12}c_{23}(-w_{32}\sqrt{1-w^2_{21}} - w_{21}w_{31}\sqrt{1-w^2_{32}}) + \sqrt[4]{\Delta m^2_{31}}s_{23}\sqrt{(1-w^2_{31})(1-w^2_{32})}e^{i\Phi_2/2}|^2, \quad \text{(B20)}$$

$$M_3|V_{\tau 3}|^2 \approx |\sqrt[4]{\Delta m^2_{21}}c_{12}s_{23}(-w_{32}\sqrt{1-w^2_{21}} - w_{21}w_{31}\sqrt{1-w^2_{32}}) - \sqrt[4]{\Delta m^2_{31}}\sqrt{(1-w^2_{31})(1-w^2_{32})}e^{i\Phi_2/2}|^2. \quad \text{(B21)}$$

(ii) *Inverted hierarchy.*—Under the approximations $m_3 \approx 0$ and $s_{13} = 0$, we have

$$M_1|V_{e1}|^2 \approx |\sqrt[4]{\Delta m^2_{21} + |\Delta m^2_{31}|}s_{12}w_{21}\sqrt{1-w^2_{31}} + \sqrt[4]{|\Delta m^2_{31}|}c_{12}\sqrt{(1-w^2_{31})(1-w^2_{21})}e^{i\Phi_1/2}|^2, \quad \text{(B22)}$$

$$M_1|V_{\mu 1}|^2 \approx |\sqrt[4]{\Delta m^2_{21} + |\Delta m^2_{31}|}c_{12}c_{23}w_{21}\sqrt{1-w^2_{31}} - \sqrt[4]{|\Delta m^2_{31}|}s_{12}c_{23}\sqrt{(1-w^2_{21})(1-w^2_{31})}e^{i\Phi_1/2}|^2, \quad \text{(B23)}$$

$$M_1|V_{\tau 1}|^2 \approx |\sqrt[4]{\Delta m^2_{21} + |\Delta m^2_{31}|}c_{12}s_{23}w_{21}\sqrt{1-w^2_{31}} - \sqrt[4]{|\Delta m^2_{31}|}s_{12}s_{23}\sqrt{(1-w^2_{21})(1-w^2_{31})}e^{i\Phi_1/2}|^2. \quad \text{(B24)}$$

$$M_2|V_{e2}|^2 \approx |\sqrt[4]{\Delta m^2_{21} + |\Delta m^2_{31}|}s_{12} \times (-w_{21}w_{31}w_{32} + \sqrt{(1-w^2_{21})(1-w^2_{32})}) + \sqrt[4]{|\Delta m^2_{31}|}c_{12}(-w_{31}w_{32}\sqrt{1-w^2_{21}} - w_{21} \times \sqrt{1-w^2_{32}})e^{i\Phi_1/2}|^2, \quad \text{(B25)}$$

$$M_2|V_{\mu 2}|^2 \approx |\sqrt[4]{\Delta m^2_{21} + |\Delta m^2_{31}|}c_{12}c_{23} \times (-w_{21}w_{31}w_{32} + \sqrt{(1-w^2_{21})(1-w^2_{32})}) - \sqrt[4]{|\Delta m^2_{31}|}s_{12}c_{23}(-w_{31}w_{32}\sqrt{1-w^2_{21}} - w_{21}\sqrt{1-w^2_{32}})e^{i\Phi_1/2}|^2, \quad \text{(B26)}$$

$$M_2|V_{\tau 2}|^2 \approx |\sqrt[4]{\Delta m^2_{21} + |\Delta m^2_{31}|}c_{12}s_{23} \times (-w_{21}w_{31}w_{32} + \sqrt{(1-w^2_{21})(1-w^2_{32})}) - \sqrt[4]{|\Delta m^2_{31}|}s_{12}s_{23}(-w_{31}w_{32}\sqrt{1-w^2_{21}} - w_{21}\sqrt{1-w^2_{32}})e^{i\Phi_1/2}|^2. \quad \text{(B27)}$$

$$M_3|V_{e3}|^2 \approx |\sqrt[4]{\Delta m^2_{21} + |\Delta m^2_{31}|}s_{12} \times (-w_{32}\sqrt{1-w^2_{21}} - w_{21}w_{31}\sqrt{1-w^2_{32}}) + \sqrt[4]{|\Delta m^2_{31}|}c_{12}(w_{21}w_{32} - w_{31} \times \sqrt{(1-w^2_{21})(1-w^2_{32})})e^{i\Phi_1/2}|^2, \quad \text{(B28)}$$

$$M_3|V_{\mu 3}|^2 \approx |\sqrt[4]{\Delta m^2_{21} + |\Delta m^2_{31}|}c_{12}c_{23} \times (-w_{32}\sqrt{1-w^2_{21}} - w_{21}w_{31}\sqrt{1-w^2_{32}}) - \sqrt[4]{|\Delta m^2_{31}|}s_{12}c_{23}(w_{21}w_{32} - w_{31} \times \sqrt{(1-w^2_{21})(1-w^2_{32})})e^{i\Phi_1/2}|^2, \quad \text{(B29)}$$

$$M_3|V_{\tau 3}|^2 \approx |\sqrt[4]{\Delta m^2_{21} + |\Delta m^2_{31}|}c_{12}s_{23} \times (-w_{32}\sqrt{1-w^2_{21}} - w_{21}w_{31}\sqrt{1-w^2_{32}}) - \sqrt[4]{|\Delta m^2_{31}|}s_{12}s_{23}(w_{21}w_{32} - w_{31} \times \sqrt{(1-w^2_{21})(1-w^2_{32})})e^{i\Phi_1/2}|^2. \quad \text{(B30)}$$

APPENDIX C: $U(1)_{B-L}$ AND $U(1)_X$ EXTENSIONS OF THE STANDARD MODEL

It is well-known that $B - L$ is an accidental global symmetry in the standard model and its origin is unknown.

In order to understand the origin of Majorana neutrino masses it is crucial to look for new scenarios where $B-L$ can be spontaneously broken. Here we focus on a simple extension of the standard model where $U(1)_{B-L}$ is a local symmetry and in order to cancel the anomalies one has to introduce three right-handed neutrinos. Therefore, this model is based on the gauge symmetry $SU(3)_C \times \bigoplus SU(2)_L \bigoplus U(1)_Y \bigoplus U(1)_{B-L}$ [6]. The matter fields have the following properties:

$$Q_L = \begin{pmatrix} u \\ d \end{pmatrix}_L \sim (3, 2, 1/6, 1/3), \qquad u_R \sim (3, 1, 2/3, 1/3), \qquad d_R \sim (3, 1, -1/3, 1/3), \tag{C1}$$

$$l_L = \begin{pmatrix} \nu \\ e \end{pmatrix}_L \sim (1, 2, -1/2, -1), \quad e_R \sim (1, 1, -1, -1), \quad \text{and} \quad \nu_R \sim (1, 1, 0, -1), \tag{C2}$$

where ν_R are the right-handed neutrinos. Here we use the normalization where $Q = T_3 + Y$. In order to generate the right-handed neutrino masses and break the local $B-L$ symmetry one has to add a new scalar field $S \sim (1, 1, 0, 2)$.

1. Interactions and symmetry breaking

In this context the kinetic terms for the Abelian sector are given by

$$\mathcal{L}_{\text{gauge}} = -\frac{1}{4} F^{\mu\nu} F_{\mu\nu} - \frac{1}{4} F'^{\mu\nu} F'_{\mu\nu} - \frac{\epsilon}{2} F^{\mu\nu} F'_{\mu\nu}, \tag{C3}$$

where

$$F^{\mu\nu} = \partial^\mu B^\nu - \partial^\nu B^\mu, \quad \text{and} \quad F'_{\mu\nu} = \partial_\mu B'_\nu - \partial_\nu B'_\mu. \tag{C4}$$

Here B_ν and B'_ν are the gauge fields for $U(1)_Y$ and $U(1)_{B-L}$, respectively. Since the mixing between the Abelian gauge bosons has to be very small we work in the case where $\epsilon = 0$. The kinetic terms for the matter fields read as

$$\mathcal{L}_{\text{kinetic}} = i\bar{Q}_L \gamma^\mu D_\mu Q_L + i\bar{u}_R \gamma^\mu D_\mu u_R + i\bar{d}_R \gamma^\mu D_\mu d_R + i\bar{l}_L \gamma^\mu D_\mu l_L + i\bar{e}_R \gamma^\mu D_\mu e_R + i\bar{\nu}_R \gamma^\mu D_\mu \nu_R, \tag{C5}$$

where

$$D_\mu \nu_R = \partial_\mu \nu_R - i g_{BL} B'_\mu \nu_R. \tag{C6}$$

As we have explained before the Higgs sector is composed of the SM Higgs, $H^T = (H^+, H^0)$, and an extra Higgs, $S = S_R + iS_I$, which is needed to break $B-L$. The relevant Lagrangian for the scalar fields is given by

$$\mathcal{L}_{\text{Higgs}} = (D_\mu H)^\dagger (D^\mu H) + (D_\mu S)^\dagger (D^\mu S) - V(H, S), \tag{C7}$$

where

$$D_\mu S = \partial_\mu S + i2 g_{BL} B'_\mu S. \tag{C8}$$

The gauge invariant Yukawa interactions of neutrinos are

$$-\mathcal{L}_Y^\nu = Y_\nu^D \bar{l}_L \tilde{H} \nu_R + \frac{Y_\nu^M}{2} \nu_R^T C \nu_R S + \text{H.c.} \tag{C9}$$

Once S gets the vacuum expectation value $\langle S \rangle \to v_S/\sqrt{2}$, $B-L$ is broken and one gets the mass of neutral gauge boson $Z' = Z_{B-L}$ with $M_{Z'} = 2 g_{BL} v_S$ from the second kinetic term in Eq. (C7), and the mass matrix of right-handed neutrino with $M_N = Y_\nu^M v_S/\sqrt{2}$ from Eq. (C9). In order not to upset applicability of perturbative theory, we require $Y_\nu^M \leq 1$ and get an upper bound of the mass of the heavy neutrinos $M_N \leq M_{Z'}/(2\sqrt{2} g_{BL})$.

The scalar potential is given by

$$V(H, S) = -m_H^2 H^\dagger H + \lambda_H (H^\dagger H)^2 - m_S^2 S^\dagger S + \lambda_S (S^\dagger S)^2 + a_S (H^\dagger H)(S^\dagger S), \tag{C10}$$

where all parameters are real. Notice that this scalar potential has the global symmetry $O(4)_H \bigotimes O(2)_S$. The minimization conditions in this case read as

$$0 = v_0 \left(-m_H^2 + \lambda_H v_0^2 + \frac{a_S}{2} v_S^2 \right), \tag{C11}$$

$$0 = v_S \left(-m_S^2 + \lambda_S v_S^2 + \frac{a_S}{2} v_0^2 \right). \tag{C12}$$

Notice that one can have several vacua but only the case $v_0 \neq 0$ and $v_S \neq 0$ is allowed by the experiment. Now, in order to satisfy the condition of minimum one has to satisfy the following condition:

$$\lambda_H a_S v_0^4 + 4\lambda_H \lambda_S v_0^2 v_S^2 + \lambda_S a_S v_S^4 > 0. \tag{C13}$$

The potential is bounded from below when $\lambda_H \lambda_S - a_S^2/4 > 0$. Using the minimization conditions above one can find the solution in the phenomenologically allowed case:

$$v_0^2 = \frac{2(a_S m_S^2 - 2\lambda_S m_H^2)}{a_S^2 - 4\lambda_H \lambda_S} > 0, \tag{C14}$$

$$v_S^2 = \frac{2(a_S m_H^2 - 2\lambda_H m_S^2)}{a_S^2 - 4\lambda_H \lambda_S} > 0. \tag{C15}$$

Using these conditions one can discuss different cases for the parameters in the Lagrangian. Expressing the numerators and the denominator as $n_1 = a_S m_H^2 - 2\lambda_H m_S^2$, $n_2 = a_S m_S^2 - 2\lambda_S m_H^2$, and $d = a_S^2 - 4\lambda_S \lambda_H$.

(i) Imposing $v_S^2 > 0$ one has the case $n_1 > 0$ and $d > 0$, or $n_1 < 0$ and $d < 0$.
(ii) Imposing $v_0^2 > 0$ one has $n_2 > 0$ and $d > 0$, or $n_2 < 0$ and $d < 0$.

2. Higgs bosons properties

As we have discussed before the Higgs sector of this model is composed of the SM Higgs, $H^T = (H^+, (\upsilon_0 + H^0 + i\xi^0)/\sqrt{2})$, and an extra Higgs, $S = (\upsilon_S + S^0 + iS_I)/\sqrt{2}$, which is needed to break $B - L$ and generate neutrino masses. In this context one will have only two CP-even physical Higgses h and H, and the mass matrix for the these fields is given by

$$\mathcal{M}_0^2 = \begin{pmatrix} \lambda_H \upsilon_0^2/2 - a_S \upsilon_S^2/4 & a_S \upsilon_0 \upsilon_S \\ a_S \upsilon_0 \upsilon_S & \lambda_S \upsilon_S^2/2 - a_S \upsilon_0^2/4 \end{pmatrix}. \tag{C16}$$

The physical Higgses are defined by

$$\begin{pmatrix} h \\ H \end{pmatrix} = \begin{pmatrix} \cos\theta_0 & \sin\theta_0 \\ -\sin\theta_0 & \cos\theta_0 \end{pmatrix} \begin{pmatrix} H^0 \\ S^0 \end{pmatrix}, \tag{C17}$$

where the mixing angle is

$$\tan 2\theta_0 = \frac{a_S \upsilon_0 \upsilon_S}{\lambda_H \upsilon_0^2 - \lambda_S \upsilon_S^2 + a_S(\upsilon_0^2 - \upsilon_S^2)}. \tag{C18}$$

It is easy to check that S_I is the Goldstone boson eaten by the Z' in the theory.

3. Feynman rules

We now summarize the Feynman rules for the SM with $U(1)_{B-L}$ and $U(1)_X$ extensions in Tables I and II, respectively.

4. Z' Decays in $U(1)_X$ extension

The charge of $U(1)_X$ is defined as $X = Y - 5(B - L)/4$ and due to the mixing between $U(1)_Y$ and $U(1)_X$ we have the mixing matrix of neutral gauge bosons as below

$$\begin{pmatrix} B^\mu \\ W_3^\mu \\ B'^\mu \end{pmatrix} = \begin{pmatrix} c_W & -s_W c' & s_W s' \\ s_W & c_W c' & -c_W s' \\ 0 & s' & c' \end{pmatrix} \begin{pmatrix} A^\mu \\ Z^\mu \\ Z'^\mu \end{pmatrix}, \tag{C19}$$

where $s_W(c_W) = \sin\theta_W(\cos\theta_W)$, $s'(c') = \sin(\theta')(\cos(\theta'))$, and $\tan(2\theta') = 2g_1'\sqrt{g_2^2 + g_1^2}/(g_1'^2 + 25 g_{BL}^2 \frac{\upsilon_S^2}{\upsilon_0^2} - g_2^2 - g_1^2)$. g_1' is a free gauge coupling to qualify the mixing between the two $U(1)$ gauge symmetries. One can get their mass eigenvalues as

$$M_A = 0, \tag{C20}$$

$$M_{Z,Z'} = \frac{\upsilon_0}{2}\sqrt{g_1^2 + g_2^2}\left[\frac{1}{2}\left(\frac{g_1'^2 + 25(\frac{\upsilon_S}{\upsilon_0})^2 g_{BL}^2}{g_1^2 + g_2^2} + 1\right) \mp \frac{g_1'}{\sin 2\theta' \sqrt{g_1^2 + g_2^2}}\right]^{1/2}. \tag{C21}$$

The expressions for the possible decays of the Z' are given by

$$\Gamma(Z' \to f\bar{f}) = \frac{M_{Z'}}{12\pi} C_f \left[V_f^2 \left(1 + \frac{2m_f^2}{M_{Z'}^2}\right) + A_f^2 \left(1 - \frac{4m_f^2}{M_{Z'}^2}\right)\right] \times \sqrt{1 - \frac{4m_f^2}{M_{Z'}^2}} \tag{C22}$$

$$\Gamma\left(Z' \to \sum_m \nu_m \nu_m\right) = 3\frac{M_{Z'}}{24\pi} C_\nu (X_\nu^U)^2 \tag{C23}$$

$$\Gamma(Z' \to N_m N_m) = \frac{M_{Z'}}{24\pi} C_N (X_N^U)^2 \left[1 - 4\frac{m_N^2}{M_{Z'}^2}\right]\sqrt{1 - \frac{4m_N^2}{M_{Z'}^2}} \tag{C24}$$

$$\Gamma(Z' \to W^+W^-) = \frac{\alpha M_{Z'} s'^2}{3\tan_W^2} \frac{M_{Z'}^4}{16 M_W^4} \times \left(1 + \frac{16M_W^2}{M_{Z'}^2} - \frac{68M_W^4}{M_{Z'}^4} - \frac{48M_W^6}{M_{Z'}^6}\right) \times \sqrt{1 - \frac{4M_W^2}{M_{Z'}^2}} \tag{C25}$$

$$\Gamma(Z' \to Zh) = \frac{1}{48\pi}\frac{M_{Z'}}{M_Z^2}\left[\upsilon_0 \frac{c_{\theta_0}}{4} K - \upsilon_S s_{\theta_0} K'\right]^2 \times \left[1 + 2\frac{5M_Z^2 - M_h^2}{M_{Z'}^2} + \frac{(M_Z^2 - M_h^2)^2}{M_{Z'}^4}\right] \times \sqrt{1 - 2\frac{M_Z^2 + M_h^2}{M_{Z'}^2} + \frac{(M_Z^2 - M_h^2)^2}{M_{Z'}^4}} \tag{C26}$$

$$\Gamma(Z' \to ZH) = \frac{1}{48\pi}\frac{M_{Z'}}{M_Z^2}\left[\upsilon_0 \frac{s_{\theta_0}}{4} K + \upsilon_S c_{\theta_0} K'\right]^2 \times \left[1 + 2\frac{5M_Z^2 - M_H^2}{M_{Z'}^2} + \frac{(M_Z^2 - M_H^2)^2}{M_{Z'}^4}\right] \times \sqrt{1 - 2\frac{M_Z^2 + M_H^2}{M_{Z'}^2} + \frac{(M_Z^2 - M_H^2)^2}{M_{Z'}^4}}, \tag{C27}$$

where $f = \ell,\ q,\ C_{\ell,\nu,N} = 1,\ C_q = 3$, and $V_f = (X_{f_L} + X_{f_R})/2$, $A_f = (-X_{f_L} + X_{f_R})/2$.

[1] P. Minkowski, Phys. Lett. **67B**, 421 (1977); see also T. Yanagida, in *Proceedings of the Workshop on the Unified Theory and the Baryon Number in the Universe*, edited by O. Sawada *et al.* (KEK, Tsukuba, Japan, 1979, KEK Report No. 79-18), p. 95; M. Gell-Mann, P. Ramond, and R. Slansky, in *Supergravity*, edited by P. van Nieuwenhuizen *et al.* (North-Holland, Amsterdam, 1979), p. 315; S. L. Glashow, in *Quarks and Leptons, Cargèse*, edited by M. Lévy *et al.* (Plenum, New York, 1980), p. 707; R. N. Mohapatra and G. Senjanović, Phys. Rev. Lett. **44**, 912 (1980).

[2] W. Konetschny and W. Kummer, Phys. Lett. **70B**, 433 (1977); see also T. P. Cheng and L. F. Li, Phys. Rev. D **22**, 2860 (1980); G. Lazarides, Q. Shafi, and C. Wetterich, Nucl. Phys. **B181**, 287 (1981); J. Schechter and J. W. F. Valle, Phys. Rev. D **22**, 2227 (1980); R. N. Mohapatra and G. Senjanović, Phys. Rev. D **23**, 165 (1981).

[3] R. Foot, H. Lew, X. G. He, and G. C. Joshi, Z. Phys. C **44**, 441 (1989); see also E. Ma, Phys. Rev. Lett. **81**, 1171 (1998); B. Bajc and G. Senjanović, J. High Energy Phys. 08 (2007) 014; P. Fileviez Pérez, Phys. Lett. B **654**, 189 (2007); Phys. Rev. D **76**, 071701 (2007); J. High Energy Phys. 03 (2009) 142.

[4] A. Zee, Phys. Lett. **93B**, 389 (1980); **95B**, 290 (1980); K. S. Babu, Phys. Lett. B **203**, 132 (1988); K. S. Babu and C. Macesanu, Phys. Rev. D **67**, 073010 (2003); C. S. Chen, C. Q. Geng, and J. N. Ng, Phys. Rev. D **75**, 053004 (2007).

[5] P. Fileviez Pérez and M. B. Wise, Phys. Rev. D **80**, 053006 (2009).

[6] See for example E. D. Carlson, Nucl. Phys. **B286**, 378 (1987).

[7] W. Y. Keung and G. Senjanovic, Phys. Rev. Lett. **50**, 1427 (1983); D. A. Dicus, D. D. Karatas, and P. Roy, Phys. Rev. D **44**, 2033 (1991); A. Datta, M. Guchait, and A. Pilaftsis, Phys. Rev. D **50**, 3195 (1994); F. M. L. Almeida, Y. D. A. Coutinho, J. A. Martins Simoes, and M. A. B. do Vale, Phys. Rev. D **62**, 075004 (2000); O. Panella, M. Cannoni, C. Carimalo, and Y. N. Srivastava, Phys. Rev. D **65**, 035005 (2002).

[8] T. Han and B. Zhang, Phys. Rev. Lett. **97**, 171804 (2006); F. del Aguila and J. A. Aguilar-Saavedra, Nucl. Phys. **B813**, 22 (2009); W. Chao, Z. G. Si, Z. z. Xing, and S. Zhou, Phys. Lett. B **666**, 451 (2008); S. Bar-Shalom, G. Eilam, T. Han, and A. Soni, Phys. Rev. D **77**, 115019 (2008); A. Atre, T. Han, S. Pascoli, and B. Zhang, J. High Energy Phys. 05 (**2009**) 030; J. Kersten and A. Y. Smirnov, Phys. Rev. D **76**, 073005 (2007); F. del Aguila, J. A. Aguilar-Saavedra, and R. Pittau, J. High Energy Phys. 10 (2007) 047; S. Blanchet, Z. Chacko, and R. N. Mohapatra, Phys. Rev. D **80**, 085002 (2009).

[9] See for example K. Huitu, S. Khalil, H. Okada, and S. K. Rai, Phys. Rev. Lett. **101**, 181802 (2008); J. A. Aguilar-Saavedra, arXiv:0905.2221; L. Basso, A. Belyaev, S. Moretti, and C. H. Shepherd-Themistocleous, Phys. Rev. D **80**, 055030 (2009).

[10] See an alternative formulation with heavy neutrino couplings to the SM Z-boson, P. Q. Hung, Phys. Lett. B **649**, 275 (2007).

[11] B. Pontecorvo, Zh. Eksp. Teor. Fiz. **33**, 549 (1957); **34**, 247 (1958); **53**, 1717 (1967); Z. Maki, M. Nakagawa, S. Sakata, Prog. Theor. Phys. **28**, 870 (1962).

[12] J. A. Casas and A. Ibarra, Nucl. Phys. **B618**, 171 (2001).

[13] T. Schwetz, M. Tortola, and J. W. F. Valle, New J. Phys. **10**, 113011 (2008).

[14] M. C. Gonzalez-Garcia and M. Maltoni, Phys. Rep. **460**, 1 (2008).

[15] M. Flanz, E. A. Paschos, U. Sarkar, and J. Weiss, Phys. Lett. B **389**, 693 (1996); A. Pilaftsis, Phys. Rev. D **56**, 5431 (1997); A. Pilaftsis and T. E. J. Underwood, Nucl. Phys. **B692**, 303 (2004); W. Buchmuller, R. D. Peccei, and T. Yanagida, Annu. Rev. Nucl. Part. Sci. **55**, 311 (2005); W. Buchmuller, P. Di Bari, and M. Plumacher, Ann. Phys. (N.Y.) **315**, 305 (2005).

[16] S. Blanchet, Z. Chacko, S. S. Granor, and R. N. Mohapatra, arXiv:0904.2174.

[17] P. Fileviez Pérez, T. Han, G. Y. Huang, T. Li, and K. Wang, Phys. Rev. D **78**, 071301 (2008); **78**, 015018 (2008).

[18] P. Langacker, Rev. Mod. Phys. **81**, 1199 (2009).

[19] M. S. Carena, A. Daleo, B. A. Dobrescu, and T. M. P. Tait, Phys. Rev. D **70**, 093009 (2004); F. Petriello and S. Quackenbush, Phys. Rev. D **77**, 115004 (2008).

[20] J. Pumplin, D. R. Stump, J. Huston, H. L. Lai, P. M. Nadolsky, and W. K. Tung (CTEQ Collaboration), J. High Energy Phys. 07 (2002) 012.

[21] J. Alwall, P. Demin, S. d. Visscher, R. Frederix, M. Herquet, F. Maltoni, T. Plehn, D. L. Rainwater, and T. Stelzer, J. High Energy Phys. 09 (2007) 028.

[22] CMS Collaboration, "*CMS Physics, Technical Design Report, V.2: Physics Performance*," CERN Report No. CERN-LHCC-2006-021 2006 (unpublished).